Nano Research Energy

ISSN 2791-0091 (print); 2790-8119 (online)
https://doi.org/10.26599/NRE.2025.9120194

Review Article

Recent progress in host and electrolyte engineering towards Li_2S cathode for lithium-sulfur battery

Wang Xi[1,§], Song Zhifan[1,§], Liu Runqiu[1], Yu Ranbo[1,2] (✉), and Wang Jiangyan[3,4] (✉)

[1] School of Metallurgical and Ecological Engineering, University of Science and Technology Beijing, Beijing 100083, China
[2] College of Chemistry and Environmental Engineering, Shenzhen University, Shenzhen 518071, China
[3] State Key Laboratory of Biopharmaceutical Preparation and Delivery, Institute of Process Engineering, Chinese Academy of Sciences, Beijing 100190, China
[4] School of Chemical Engineering, University of Chinese Academy of Sciences, Beijing 100049, China
[§] Wang Xi and Song Zhifan contributed equally to this work.

Received: 23 June 2025 / **Revised:** 13 July 2025 / **Accepted:** 28 August 2025 / **Published date:** 31 December 2025

ABSTRACT

Lithium sulfide (Li_2S) has drawn much attention owing to its super-high theoretical specific capacity and energy density, as well as its compatibility with lithium-free anode materials. However, the commercialization of Li_2S cathode is severely hindered by its poor rate capability and short cyclic life arising from its poor electrical conductivity, high activation energy barrier and shuttle effect of polysulfide intermediates. Many approaches have been reported, mainly focusing on the development of host for Li_2S cathode as well as electrolyte engineering, which have achieved great progress. This review firstly provides an in-depth discussion of the challenges encountered Li_2S cathode, subsequently discusses the host design for Li_2S cathode and electrolyte engineering, focusing on the fundamental mechanism underlying the host or electrolyte engineering for improving the reaction kinetics and interface stability. Finally, the remaining challenges and future directions of Li_2S cathode are discussed to further improve the performance of Li_2S cathode materials and promote their practical application.

KEYWORDS

lithium sulfide, host design, electrolyte engineering, reaction kinetics, interface stability

1 Introduction

In various energy storage systems, lithium-sulfur batteries (LSBs), which utilize sulfur (S) or lithium sulfide (Li_2S) as the cathode material, have garnered increasing attention due to their super-high theoretical energy density of 2600 $Wh{\cdot}kg^{-1}$ [1–5]. Compared to S cathode, Li_2S cathode possesses multiple advantages and has emerged as a promising cathode candidate for next-generation lithium rechargeable batteries (Fig. 1). Firstly, Li_2S delivers a high theoretical specific capacity of 1166 $mAh{\cdot}g^{-1}$ and avoid large volume expansion during lithiation process unlike S cathode [6–9]. Secondly, while S is highly volatile and can sublimate above 100 °C, Li_2S possesses a relatively high melting point of 938 °C [10, 11]. The excellent thermal stability of Li_2S enables its synthesis from diverse precursors (such as Li_2SO_4 and Li) through different high-temperature reactions, which ensures the uniform distribution and good contact of Li_2S with host materials [12]. Moreover, Li_2S is compatible with lithium-free anode materials such as graphite, silicon, and tin, thus avoiding the safety issues associated with lithium metal [13–17].

Nevertheless, LSBs using Li_2S as the cathode material also encounter several challenges. During the charge and discharge process, intermediate product Li_2S_x ($4 \le x \le 8$) is highly soluble in ether-based lithium sulfur electrolytes and can diffuse to the anode, resulting in the loss of active materials and a reduced cycle life [3, 18–21]. In addition, Li_2S is highly sensitive to moisture in the air and will react with water to produce the toxic hydrogen sulfide, necessitating preservation and processing in an inert atmosphere, which increases the cost and complexity of Li_2S processing compared to sulfur [6, 22, 23]. Thirdly, similar to sulfur, Li_2S exhibits very poor electronic and ionic conductivity, which slows the initial solid-solid reaction kinetics [18, 24–26]. Therefore, the charge transfer resistance at the Li_2S cathode/electrolyte interface is very high, leading to a high energy barrier of ~ 1 V during the initial charging process. The high barrier requires a high voltage to achieve full delithiation of Li_2S , resulting in potential electrolyte decomposition, poor cyclic performance, and low energy efficiency [27–29].

In response to these issues, studies have demonstrated that the above challenges can be solved by making Li_2S composites with other host materials and through electrolyte additive engineering

Address correspondence to Yu Ranbo, ranbo_yu@163.com; Wang Jiangyan, jywang@ipe.ac.cn

(Fig. 2). The rational design of host materials has emerged as a critical strategy to address Li_2S intrinsic limitations. Various host materials have been reported. Carbon-based hosts demonstrate exceptional electrical conductivity and polysulfide confinement. Metal compounds hosts offer strong chemisorption and catalytic effects to mitigate "shuttle effect", while the conductive polymer can improve the conductivity of Li_2S, and also use its functional group to adsorb polysulfide so that slow down the "shuttle effect". In addition to host adoption, electrolyte engineering, which is mainly through the addition of electrolyte additives, e.g., redox mediators (RMs), which facilitate *in-situ* electron transport by shortening the intrinsic transport path of Li_2S, thus improving cathode capacity retention and rate capability.

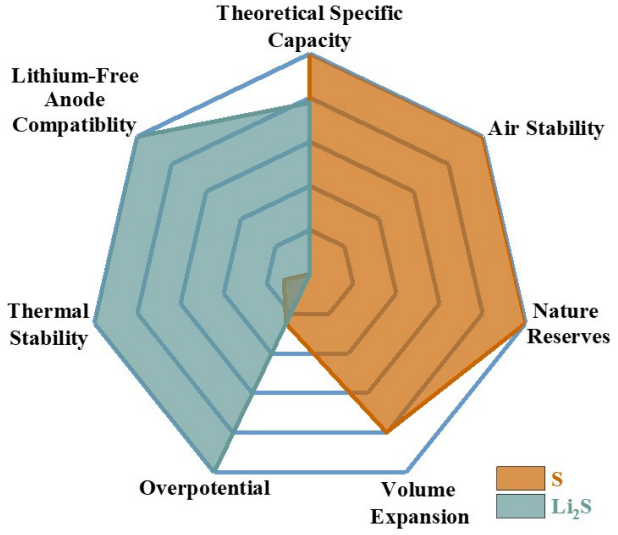

Figure 1 Radar comparison chart of S and Li_2S cathode.

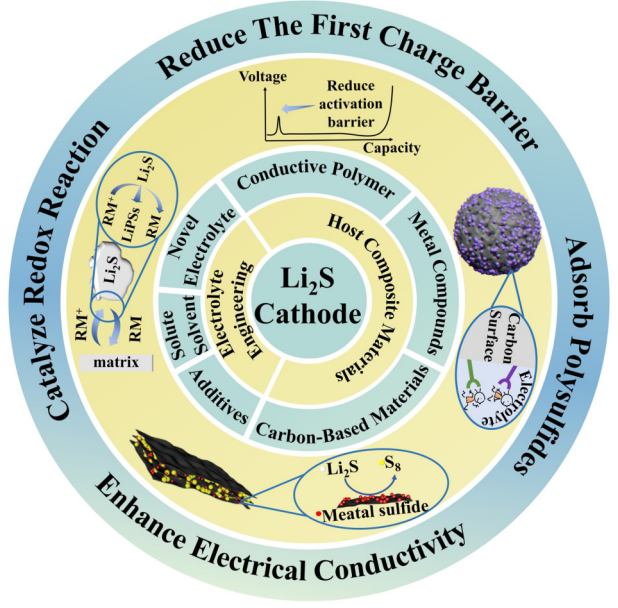

Figure 2 Schematic diagram of modification methods to address the challenges of Li_2S cathode.

Figure 3 summarizes the papers about Li_2S cathode published during the past decade. Obviously, great efforts have been devoted to Li_2S cathode. Some reviews have summarized the advancements of Li_2S, including host design and electrolyte engineering. In this Review, by deeply understanding the crucial challenges of Li_2S cathode, we mainly focus on the discussion of the fundamental mechanism underlying the host or electrolyte engineering for improving the reaction kinetics and interface stability of Li_2S cathode. In view of the beneficial effects of host materials on Li_2S cathode, the reaction kinetics of Li_2S are significantly improved through their complementary functionalities including high electrical conductivity, and good catalytic effect, while the interface stability is effectively improved through both the physical trapping and chemical adsorption function of hosts. In view of electrolyte engineering, we introduce RMs which facilitate *in-situ* electron transport by shortening the intrinsic transport path of Li_2S, thereby amplifying kinetics gains. Meanwhile, altering the solute-solvent composition alleviates corrosive attack on the electrode surface, stabilizing its structure over extended cycling. Solid-state electrolytes eliminate the mass-transfer limitations at conventional solid-liquid interfaces, thus suppressing polysulfide dissolution, enhancing interfacial stability, and eliminating electrolyte leakage. Collectively, these synergistic advances establish a solid foundation for practical, high-performance LSBs using Li_2S cathodes. In the final section, remained challenges and vision for future research work is outlined. In addition, the development of practical technologies based on Li_2S cathode materials in the near future is also highlighted.

2 Challenges

As previously discussed, the Li_2S cathode material exhibits poor conductivity. During the charge and discharge process, the

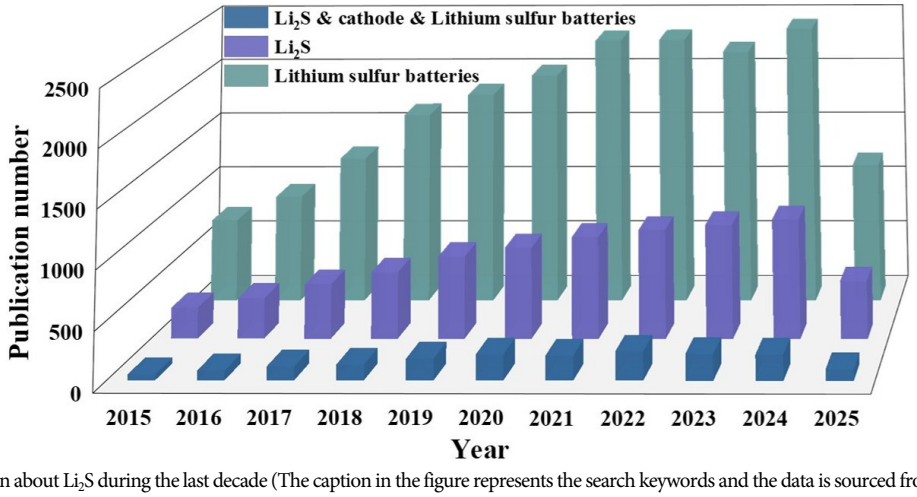

Figure 3 The publication about Li_2S during the last decade (The caption in the figure represents the search keywords and the data is sourced from Web of Science).

intermediate Li_2S_x dissolves readily in electrolyte, leading to the loss of active materials because of the shuttle effect, which result in decreased battery capacity and Coulomb efficiency. Additionally, the reactive nature of Li_2S in air will complicate its practical application. Another critical challenge in Li_2S application is the requirement for a high charge cut-off voltage during the initial charging process to fully activate. As shown in Fig. 4, Li_2S exhibits a high activation barrier during the first charge, followed by a long charging platform, indicating that two reactions are involved in the initial charging process. The high barrier is related to the nucleation process of the phase, necessitating additional energy drive [30, 31]. It has been shown that the existence of the barrier is related to the complementary nucleation of polysulfides during the oxidation of Li_2S. During the first charge, polysulfides do not form until the activation barrier is reached. The monophasic reaction (Li_2S (s) → $Li_{2-x}S$ (s) + xLi^+ + xe^-) proceeds up to the barrier, after which a polysulfide phase is formed during a long plateau. In the platform area of the first charge, the two opposing reactions become dominate [30]. Factors affecting the activation barrier level generally include: (I) charge transfer between substances, (II) diffusion of lithium ions within Li_2S, and (III) electronic conductivity of the Li_2S cathode material. The slow charge transfer process between Li_2S and electrolyte before polysulfide nucleation is the main factor for Li_2S to form a high activation barrier during the initial charging process [25]. The limited lithium-ion diffusion within Li_2S is another fundamental obstacle. At the initial stage of charging, the process involving a single-phase reaction is confined to the triple-phase boundary where Li_2S, conductive carbon, and electrolyte meet, restricting lithiation/delithiation to the Li_2S particle surface and requiring lithium ions to diffuse through the Li_2S particle [30, 32]. Still, Li_2S faces some problems that need to be addressed before its commercialization in Li-S batteries.

3 Host material engineering for Li_2S cathode

By utilizing host materials to develop Li_2S-based composite cathode materials, such as Li_2S/carbon, Li_2S/metal compounds, and Li_2S/conductive polymers, the above set of issues can be effectively solved. Due to the kinetic interface increases, the reaction kinetics is improved because Li_2S and the conductive host material are fully in contact. In the following part, the progress of Li_2S-based composite cathode materials is discussed deeply.

3.1 Li_2S/carbon composite cathode materials

Researchers have addressed the challenges associated with Li_2S by integrating it with other materials to form composites. Carbon materials were among the first to be used due to the ability to alleviate their inherent issues [33]. First of all, carbon materials possess excellent electrical conductivity, providing an effective electronic network to the active material, which facilitates electron transfer from the collector to the active material, lowering the energy required to initiate electrochemical reactions [34–37]. Secondly, carbon materials exhibit superior mechanical properties, enabling them to maintain their structural integrity during multiple cycles [34, 38–40]. Thirdly, carbon materials can be synthesized into various dimensional forms, such as 1D carbon nanotubes [41–43] and nanowires [41, 42], 2D sheets [44–46], 3D spheres [47–55] or layered stacks [56, 57], which can contribute to the construction of more universal electrode, thus enhancing electrolyte infiltration and ion diffusion kinetics, and optimizing interfacial charge transfer at reduced overpotentials. Fourthly, closed carbon materials that are easy to synthesize can use their internal cavities to store active materials while also absorbing and trapping polysulfides, thereby preventing the shuttle effect [22, 31, 44, 52, 53]. Fifthly, the surface of carbon materials can also be functionalized by adding certain elements to enhance their interaction with polysulfides [58–61], thereby hindering the loss of active substances and alleviating the shuttle effect, stabilizing charge transfer processes and decreasing activation energy [62]. Therefore, the structure, morphology and electronic conductivity of Li_2S cathodes can be systematically optimized by synthesizing Li_2S/Carbon Composites. Researchers have conducted detailed studies on Li_2S by binding it to different conductive carbons. Among the published studies on Li_2S/Carbon Composites, several have reported notable successes in the synthesis of high-performance Li_2S/Carbon Composites.

3.1.1 *Li_2S/graphene&graphene-derivatives based composite*

Similar to traditional sulfur/carbon cathode materials, graphene materials are often combined with Li_2S to form Li_2S/carbon composite cathode materials. Li et al. [11] synthesized

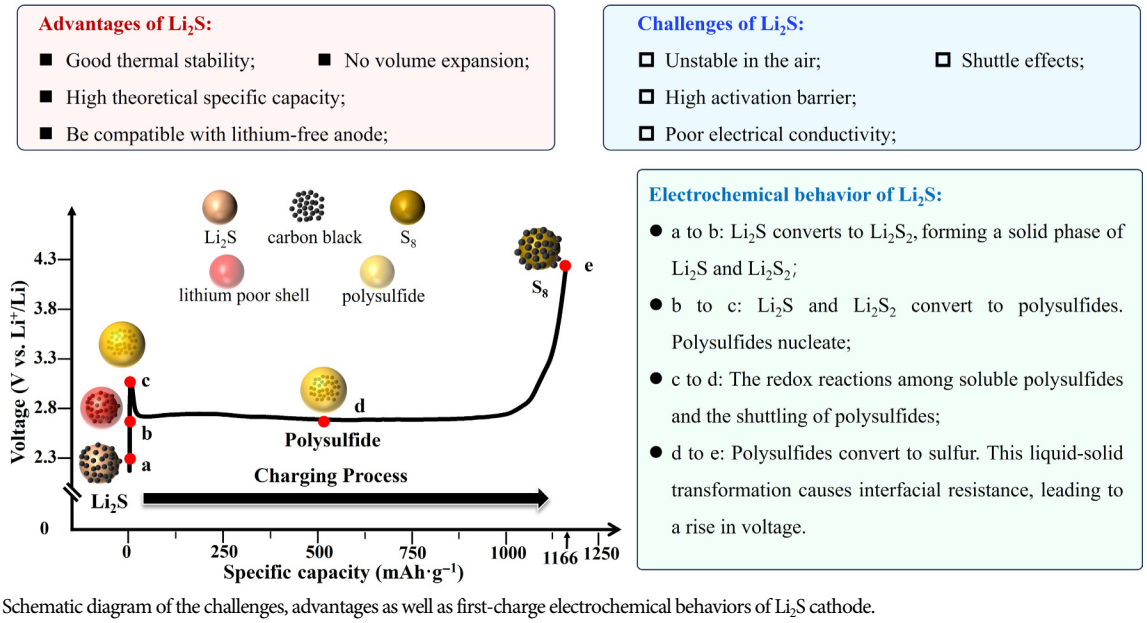

Figure 4 Schematic diagram of the challenges, advantages as well as first-charge electrochemical behaviors of Li_2S cathode.

Li_2S/graphene composites by directly pyrolyzing graphene nanoplatelet aggregates (GNAs) and lithium sulfate (Li_2SO_4), employing a simple, low-cost, scalable, and environmentally friendly method. In this process, a portion of the GNAs acts as a reducing agent to convert Li_2SO_4 to Li_2S, while the remainder is *in-situ* etched into graphene sheets to form highly conductive two-dimensional (2D) host materials that encapsulate Li_2S and improve its electrical conductivity. The *in-situ* graphene sheet is in full contact with the lithium sulfide, which takes advantage of the high electrical conductivity of carbon to enhance the reaction kinetics. As a result, this unique structure exhibits lower activation energy, better cycling performance, and higher rate capacity compared to commercial Li_2S/GNAs mixtures. Graphene with higher electrical conductivity plays a pivotal role in reducing charge transfer resistance, an effect that becomes more effective in systems with smaller particle size. For example, Wu et al. [63] reported a simple solution-based method to synthesize Li_2S/graphene composites without generating toxic gases during the synthesis process (Fig. 5(a)). Figure 5(b) shows that many Li_2S particles aggregate and interconnect due to the evaporation of the ethanol solution and subsequent sintering at 400 °C. Transmission electron microscopy (TEM) provides a clearer view of the shape and size of the particles, revealing Li_2S particles as small as 5 nm on the graphene surface. Li_2S nanoparticles embedded within the graphene matrix exhibit shortened Li^+ diffusion distance and enhanced electrochemical performance. In addition to the inherent high conductivity of graphene, this configuration promotes uniform nanoparticle distribution and enables controllable size effects. Similarly, the uniform dispersion of Li_2S on graphene allows the formation of an additional protective carbon layer during subsequent chemical vapor deposition, synthesizing typical carbon-coated Li_2S/graphene composites (Li_2S/G@C) [48]. The carbon layer not only provides space to accommodate Li_2S and alleviate the volume expansion but also prevents the dissolution of polysulfides during cycling. Additionally, graphene as a highly conductive substrate can facilitate electron transport in composite materials. After 1000 cycles at 2 C, the Li_2S could still maintain a capacity of 314 mAh·g^{-1}, which is significantly higher than that of other lithium-ion batteries.

In addition to graphene, graphene oxide (GO) is frequently utilized in combination with Li_2S. GO can anchor polysulfides to the cathode through its functional groups, such as hydroxyl, epoxide, carbonyl, and carboxyl, thus mitigating the "shuttle effect". Lin et al. [64] synthesized multi-layer carbon-coated Li_2S by mixing the prepared carbon-coated nano Li_2S (Nano Li_2S@C) with GO. The inner carbon shell prevents direct contact between the inner nano Li_2S and the liquid electrolyte, thereby enhancing the performance and cycle life of LSBs, while the outer GO chemically immobilizes polysulfides in the cathode through its functional groups, slowing their shuttling between the anode and cathode, improving the cycling stability and suppressing capacity decay. At a C/10 rate, the initial specific discharge capacity is 1263 mAh·g^{-1} (normalized to sulfur), with a capacity retention of 65.4% after 200 cycles. Hwa et al. [65] also created a composite material using a double layer of carbon and Li_2S, embedding GO

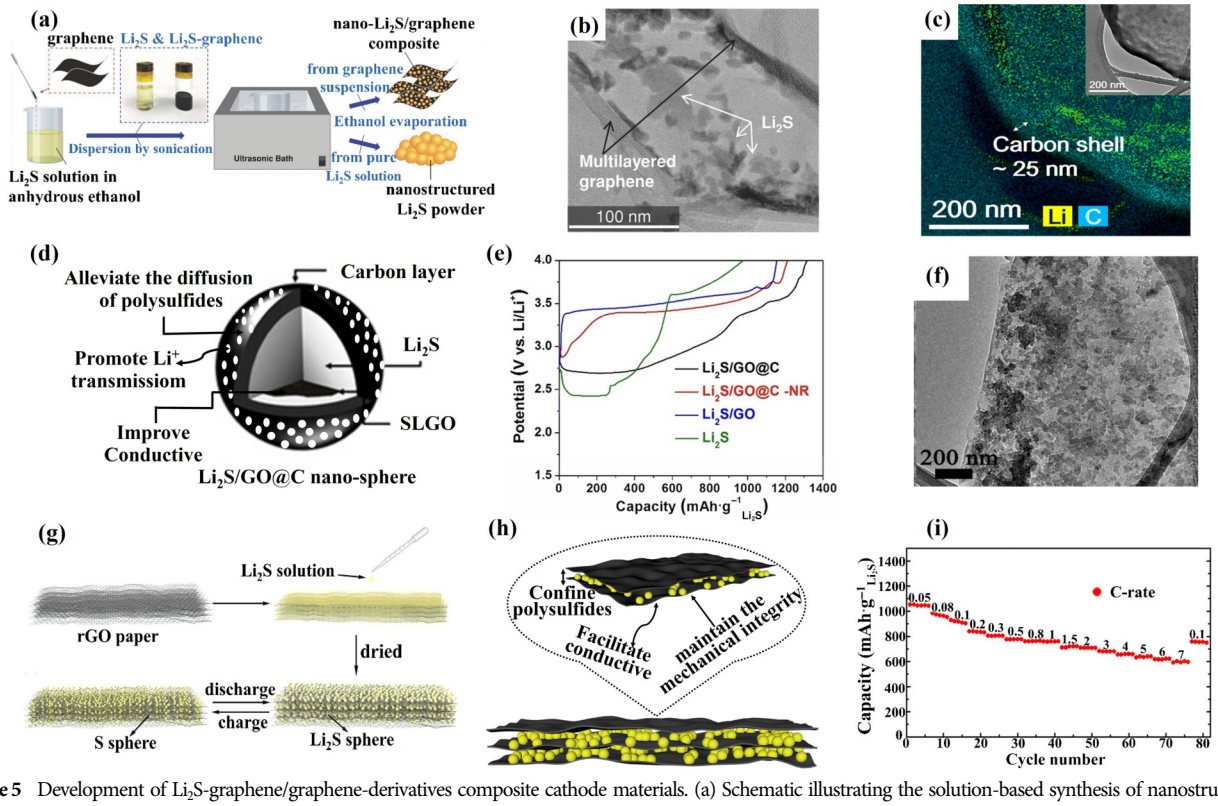

Figure 5 Development of Li_2S-graphene/graphene-derivatives composite cathode materials. (a) Schematic illustrating the solution-based synthesis of nanostructured Li_2S and Li_2S-graphene composites. (b) TEM images reveal Li_2S nanoparticles with varied morphologies anchored on graphene sheets. Reproduced with permission from Ref. [63], © 2014 WILEY-VCH Verlag GmbH & Co. KGaA, Weinheim. (c) EFTEM elemental mapping (inset: zero-loss image) confirming the uniform distribution of Li_2S/GO@C components. (d) Schematic illustration of the Li_2S/GO@C nanospheres structure and function. (e) Voltage profiles of synthesized Li_2S, Li_2S/GO, Li_2S/GO@C-NR and Li_2S/GO@C electrode at the first charge. (c) and (e) were reproduced with permission from Ref. [65], © 2015 American Chemical Society. (f) TEM image of the nano Li_2S/rGO composite. (g) Fabrication steps for nano Li_2S/rGO paper and its structural evolution during cycling. (h) Functional schematic diagram of nano Li_2S/rGO paper. (i) Rate capability of the nano Li_2S/rGO electrode at current densities ranging from 0.05 to 7 C. (f-i) were reproduced with permission from Ref. [56], © 2015 American Chemical Society.

within Li_2S and coating the outermost layer with carbon (Fig. 5(c)). The outer carbon shell can not only alleviate the volume expansion of Li_2S but also prevent Li_2S from directly contacting with the liquid electrolyte, thereby preventing polysulfides from dissolving into the electrolyte. Additionally, it serves as an electrical pathway, obviously enhancing reaction kinetics and reducing the electrode resistance. The inner GO layer fixes sulfur or polysulfides due to its functional groups; should the outer carbon layer rupture, the internal polysulfides would form chemical bonds with GO, preventing dissolution and the associated "shuttle effect". This excellent structure endows the Li_2S/GO@C electrode with a low capacity decay rate of 0.046% per cycle over 1500 cycles and a coulombic efficiency exceeding 99.5%. In addition, the outermost porous carbon provides a Li^+ transport path, and the internal GO and Li_2S fully contact, enhancing the conductivity of Li_2S (Fig. 5(d)), which enables the Li_2S/GO@C composite material to have the minimum overpotential during the first charge (Fig. 5(e)). Furthermore, Seh et al. [66] used *ab initio* simulations to demonstrate that oxygen-containing functional groups can strongly bind to polysulfides through Li-O interactions. They employed lightly oxidized GO as the packaging material for the Li_2S cathode. The Li-O interaction facilitated coating of Li_2S with GO, helping to slow the dissolution of intermediate lithium polysulfides in the electrolyte. The Li_2S/GO composite cathode exhibited cyclic stablility at 0.2 C, with an initial capacity of 782 $mAh·g^{-1}$ and an average Coulombic efficiency of 97% over 150 cycles.

Additionally, composite host materials have been explored using reduced graphene oxide (rGO) and Li_2S. rGO, typically obtained as a flexible, multilayered paper featuring a large surface area, high electronic conductivity, and strong solvent absorption, which effectively hosts nanosized Li_2S particles and enhances their utilization. Moreover, the flexibility and mechanical stability of rGO can mitigate volume changes during charging and discharging. Han et al. [67] encapsulated Li_2S derived from the thermal decomposition of Li_2S_6 within a 3D rGO network to obtained Li_2S/rGO. The large surface area and high conductivity of rGO address the poor electrical conductivity of Li_2S, which provides good contact so that enhance the reaction kinetics. Scanning electron microscopy (SEM) and other characterization methods revealed that 20–40 nm Li_2S particles are uniformly dispersed between rGO sheets. When assembled into a battery with an electrolyte containing $LiNO_3$ and polysulfide, the Li_2S/rGO nanocomposite showed a high initial capacity of 982 $mAh·g^{-1}$.

Although subsequent cycles showed a significant capacity decrease possibly due to polysulfides dissolution and shuttle mechanism, a capacity of 315 $mAh·g^{-1}$ was still abtained after 100 cycles, with a coulombic efficiency of 90%–95%. The inherent flexibility of rGO further enables its integration into binder-free electrodes and flexible devices. Wang et al. [56] used a drip coating method to deposit Li_2S solution onto the rGO paper to prepare a flexible and binder-free nano Li_2S/rGO cathode paper (Fig. 5(g)). The addition of rGO limited Li_2S particle size to 25–50 nm (Fig. 5(f)), which is much smaller than the coarse Li_2S particles without rGO. The integrated Li_2S/rGO paper takes advantage of the excellent electrical conductivity, flexibility and strong solvent absorption of the rGO paper, allowing it to be used directly as the cathode without any binders or metal substrates (Fig. 5(h)). This special structure endows the Li_2S/rGO cathode material with small activation barrier and excellent rate performance (Fig. 5(i)), achieving a high reversible capacity of 597 $mAh·g^{-1}$ even at a high rate of 7 C. Similar to the double-carbon layer Li_2S composite structures prepared using GO and other carbon layers, Wang et al. [68] used liquid phase evaporation coating with polyvinylpyrrolidone (PVP) carbonization to uniformly embed Li_2S@C particles into 3D-rGO, forming a binder-free 3D-rGO-Li_2S@C cathode. The composite structures take advantage of the high conductivity of the rGO framework to improve the electron and ion transfer rates and uses the outer carbon coating on Li_2S to inhibit the "shuttle effect" of polysulfides, further improving the overall electrochemical performance of the battery. The excellent structures of the 3D-rGO-Li_2S@C cathode provided a high initial discharge capacity of 856 $mAh·g^{-1}$ at 0.1 C. After 200 cycles at 1 C, it delivered excellent cyclic stability with a capacity of 388.4 $mAh·g^{-1}$.

With its large specific surface area, graphene can accommodate more Li_2S nanoparticles, which can improve the reaction area and further improve reaction kinetics. Meanwhile, an enhanced electron transfer rate can be obtained due to its excellent electrical conductivity. The surface of GO is rich in functional groups that can anchor polysulfides, thereby alleviating the "shuttle effect" in the charge and discharge processes. However, the relatively high cost of graphene limits its widespread applications in LSBs. Furthermore, graphene and its derivatives often suffer from reduced electrical conductivity due to incomplete reduction (for rGO) and the restacking of layered structures. Consequently, the use of graphene in Li_2S/C composite materials may not be feasible for large-scale production of Li_2S/C composite materials.

3.1.2 *Li_2S/carbon nano fiber composite*

Graphene and its derivatives are relatively expensive, and their preparation processes are complex, often leading to aggregation or stacking that reduces performance. In contrast, many studies have explored the use of carbon nanofibers (CNFs) to create composite materials with Li_2S [55, 63]. On the one hand, CNFs are easy to obtain and can be fabricated into various shapes and structures. On the other hand, compared to graphene, the raw materials for CNFs are cheap and readily available. In addition, the stable structure and large internal cavities of it can effectively store Li_2S and mitigate the "shuttle effect" of intermediate polysulfides.

Therefore, CNFs represent a promising alternative for combining with Li_2S in composite materials. Recently, Lu et al. [69] prepared highly conductive Li_2S@C/CNT composites by integrating spray drying technology with carbothermal reduction. The composite structure comprises carbon nanotube (CNT) framework and conductive carbon black spherical particles. The carbon network provides a high-speed three-dimensional channel for electron transport, enhancing electrochemical reaction kinetics and structural stability. The SEM results showed that the Li_2S particle size in Li_2S@C/CNT ranges from 2–5 μm, which is beneficial for shortening the Li^+ transport distances. Notably, the composites incorporating CNTs exhibited a relatively lower oxidation peak potential during the initial charge process compared with the Li_2S cathode without CNTs, suggesting reduced activation barrier and improved Li_2S utilization (Fig. 6(a)). This excellent design endows the prepared Li_2S@C/CNT cathode with enhanced cycling stability (520.6 $mAh·g^{-1}$ after 200 cycles at 1 C) and rate performance (301.8 $mAh·g^{-1}$ at 5 C). Similarly, a Li_2S core-carbon shell structure with a shell composed of a CNF-CNT mixture was prepared (Fig. 6(b)) [70]. The conductive CNF-CNT shell encloses redox products, preventing the shuttle of polysulfides, and improving the conductivity of the material by providing fast electronic channels

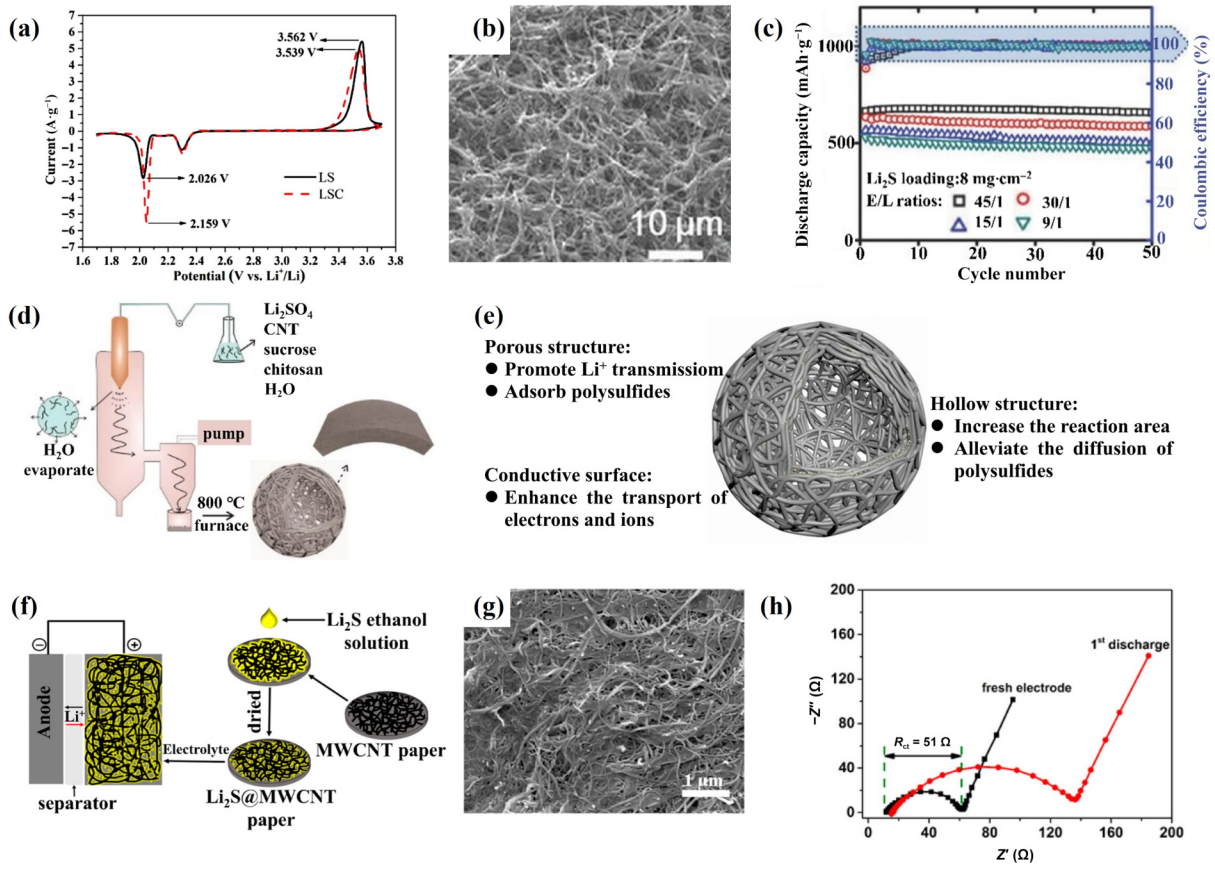

Figure 6 Development of Li_2S/carbon nanofiber composite cathode materials. (a) Comparison of CV curves in the first cycle of LS and LSC cathodes. Reproduced with permission from Ref. [69], © Lu, C. W. et al., under exclusive licence to Springer-Verlag GmbH Germany, part of Springer Nature 2024. (b) SEM image of the Li_2S cathode. (c) Cycling stability under high Li_2S mass loading. Reproduced with permission from Ref. [70], © WILEY-VCH Verlag GmbH & Co. KGaA, Weinheim 2017. (d) Synthesis pathway for Li_2S/CNT/C-N/O composite. (e) Functional schematic diagram of Li_2S/CNT/C-N/O composite. (d) was reproduced with permission from Ref. [71], © Elsevier B.V. 2018. (f) Fabrication schematic and cell configuration of nano Li_2S/MWCNT paper electrodes. (g) SEM images of the freshly made nano Li_2S/MWCNT paper electrode. (h) Nyquist plots of nano Li_2S/MWCNT paper electrode after freshly made (black) and after first cycle (red). Reproduced with permission from Ref. [74], © American Chemical Society 2015.

and smooth ion transport to the active material core. This structure allows for high Li_2S loading up to 8 mg·cm^{-2} and a low electrolyte/Li_2S ratio of 9/1 (Fig. 6(c)). In another study, researchers used the same technology to embed nanoscale Li_2S in a nitrogen/oxygen double-doped carbon nanotubes/carbon (Li_2S/CNT/C-N/O) framework (Fig. 6(d)) [71]. Thanks to the obvious hollow structure (Fig. 6(e)), contact area between the electrolyte and the active material can be significantly increased. In addition, the N and O dopants in the composite structure promote the strong adsorption interaction of polysulfides, alleviating the "shuttle effect" of intermediates. As a result, the superior architecture endows Li_2S/CNT/C-N/O cathodes with a barrier height of only 0.08 V during the initial charge process, substantially lower than the 0.67 V observed for pristine Li_2S, underscoring the pivotal role of the interconnected pore structures between CNTs and Li_2S for fast Li^+ diffusion. Ye et al. [72] prepared a novel 1D lithium sulfide carbon nanofibers (Li_2S-C-NFs) composite by electrospinning and subsequent pyrolysis. Nanoscale Li_2S is embedded in the carbon layer, ensuring good contact with carbon and improving the electrical conductivity and electron/ion transport reaction kinetics of Li_2S. Compared to the traditional electrode materials, the Li_2S-C NFs composite demonstrated a low initial activation barrier of 2.57 V and subsequent charging voltage platform of 2.51 V providing an initial specific capacity of up to 800 mAh·g^{-1} at 0.5 C and a reversible capacity of 510 mAh·g^{-1} after 100 cycles.

Functionalized CNT such as multi-walled carbon nanotubes (MWCNTs) are also commonly used to further improve the conductivity and stability of Li_2S/C composite cathodes [6]. Firstly, MWCNTs can construct a 3D conductive network, which is beneficial for the electrochemical performance of the Li_2S electrodes. Secondly, the micropores within MWCNTs ease the diffusion of polysulfides, reducing the loss of active materials and helping to regulate the volume changes during the cycling. For instance, Wu et al. [73] pioneered the use of solution-based methods to connect nanoporous Li_2S powders through MWCNTs, significantly enhancing the conductivity of the Li_2S cathode and maximizing the utilization of nanoscale Li_2S in batteries. The interwoven MWCNTs within the electrode also maintain the electrical pathways, enlarge the active surface area during cycling, and mitigate polarization at high current densities. Further investigations into MWCNTs loading reveal that an appropriately elevated content favors the formation of finely sized Li_2S particles. Additionally, Wu et al. [74] also uniformly loaded Li_2S onto binder-free and independent MWCNT paper using Li_2S solution filtration method (Fig. 6(f)). SEM revealed Li_2S particle sizes of about 10 nm distributed within the MWCNTs (Fig. 6(g)). The small Li_2S particle size and the excellent electrical conductivity of MWCNTs result in negligible overpotential for the Li_2S/MWCNTs composite cathode during the first charge, exhibiting low impedance and excellent electrochemical

performance. As shown in Fig. 6(h), due to the good contact between nano Li_2S and MWCNTs, the initial R_{ct} of the electrode is only 51 Ω, which is attributed to the good contact between Li_2S and MWCNTs, resulting in a low initial charging overpotential.

Carbon nanofibers, synthesized by spray drying, electrospinning, and solution-based methods, have been widely used in Li_2S-based cathode materials. On one hand, judiciously engineered carbon nanofibers integrate a long-range conductive network with facile functionalization; on the other, their high tensile modulus endows them with substantial potential for binder-free, self-supporting electrodes and flexible-device applications. These methods are not only cost-effective in terms of raw materials but also straightforward and facile to execute, making them more suitable for the preparation of Li_2S/carbon composites compared to the carbon materials derived from graphene and its derivatives. However, the fabrication costs of functionalization strategies and volume expansion in flexible devices remain critical considerations in practical applications.

3.1.3 *Li_2S/porous carbon composite*

Graphene and its derivatives are costly, and while carbon nanofibers offer a solution, their low yield hinders the industrial scalability. In contrast, porous carbon (PC) can be readily derived from inexpensive and abundant carbonaceous precursors such as glucose and sucrose, offering exceptional potential for practical applications.

Zheng et al. [75] coated sulfur/microporous carbon (S/MC) composite lithium metal powder (SLMP) and applied pressure to *in-situ* form a Li_2S/microporous carbon (Li_2S/MC) film cathode. Due to the good contact between the *in-situ* lithium sulfide and porous carbon, the composite structure has excellent electrochemical properties. The specific capacity of the Li_2S/MC film cathode was maintained at about 650 mAh·g^{-1} after 900 cycles. Furthermore, when integrated with commercial graphite to assemble a full battery, the capacity remained stable at 600 mAh·g^{-1} after 150 cycles. In another study, Zhang et al. [76] Li_2S nanoparticles in an N-P co-doped carbon framework, creating a binder-free composite cathode (Figs. 7(a) and 7(b)). On one hand, the 3D structure of N and P co-doped carbon provided continuous electronic channels for lithium ions, improving electrical conductivity, and electrochemical kinetics. On the other hand, P doping promoted polysulfides capture, inhibiting the "shuttle effect" and improving the ionic conductivity of Li_2S. These advantages are evidenced by the reduced polarization under a high current density of 1 C, as shown in Fig. 7(c). As a result, the Li_2S/N,P-C composite exhibited an initial discharge specific capacity exceeding about 700 mAh·g^{-1} after 100 cycles, demonstrating excellent stability due to the catalytic effect of P doping and the strong interaction between S and P. As shown in Fig. 7(d), using inexpensive Li_2SO_4 as the lithium source, glucose can also serve as a key precursor for PC [77]. Encapsulating Li_2S within this PC matrix simultaneously improves the conductivity and reaction kinetics while mitigating volume expansion during cycling. Another advantage of Li_2S is that it can match the lithium-free anode with the lithium element contained in itself. Yang et al. [14] *in-situ* prepared Li_2S and encapsulated it within CMK-3

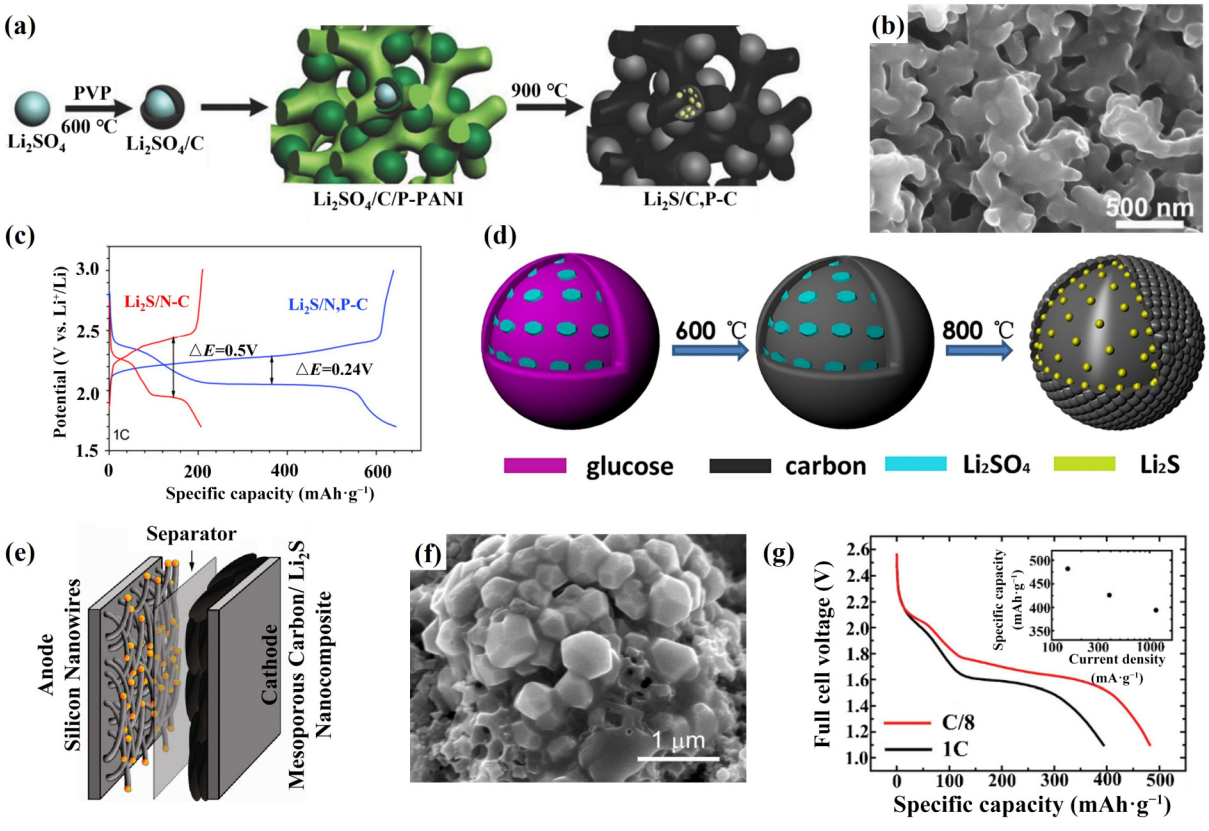

Figure 7 Development of Li_2S/porous carbon composite cathode materials. (a) Schematic representation of the synthesis process for Li_2S/N, P-C composites. (b) SEM images illustrating the morphology of Li_2S/N, P-C composites. (c) The charge–discharge profiles for Li_2S/N,P–C and Li_2S/N–C at 1 C. Reproduced with permission from Ref. [76], © 2017 WILEY-VCH Verlag GmbH & Co. KGaA, Weinheim. (d) Schematic of fabrication process of Li_2S@PC composites. Reproduced with permission from Ref. [77], © 2017 Elsevier Ltd. (e) Schematic of the Li_2S/Si battery configuration. (f) SEM image of the Li_2S/CMK-3 mesoporous carbon nanocomposite. (g) Initial discharge voltage profiles of full cells using Li_2S/CMK-3 cathodes and Si nanowire anodes, tested at rates of 1 C (1166 mA·g^{-1}) and C/8 (146 mA·g^{-1}). Inset: Rate-dependent discharge capacities at varying current densities. Reproduced with permission from Ref. [14], © 2010 American Chemical Society.

mesoporous carbon to form a full battery with silicon nanowires (Fig. 7(e)). This novel electrode design addressed issues of poor conductivity, structural changes and volume expansion caused by the use of sulfur compounds and silicon in lithium-ion batteries. As shown in Fig. 7(f), the Li_2S/CMK-3 mesoporous carbon nanocomposites had particle sizes of about 0.5–1 μm. By assembling the lithium metal-free full battery, it was found that the discharge capacity reached 482 mAh·g^{-1} at C/8 (Fig. 7(g)).

Porous carbon as a carbon source addresses the high cost of graphene and its derivatives and the low yield of carbon nanofibers. Its simple synthesis, abundant raw materials, and large pore encapsulation of Li_2S improve the electrochemical performance by inhibiting the dissolution of polysulfides and preventing the "shuttle effect", making it a promising material for industrial production.

As we discussed above, carbon introduction to Li_2S cathode can effectively lower the activation barrier. This impact could be explained as follows. Firstly, the high-conductivity carbon network provides continuous electron pathways that homogenize electron density on the Li_2S surface, suppressing localized charge accumulation during initial activation. Secondly, carbon materials with large specific surface areas enlarge the interfacial contact with Li_2S particles, shorten Li^+ diffusion distance, and reduce ion transport resistance. Finally, precisely engineered functional carbon materials exploit intrinsic defects and surface functional groups to lower the activation energy for electrochemical conversion. Although carbon materials have demonstrated abundant advantages, practical applications in LSBs still demand a careful balance between energy density and cycle life. Several critical issues may remain: (I) non-polar carbon materials possess limited mitigation for polysulfides, so the "shuttle effect" may still manifest over extended cycling; (II) the intrinsically limited capacity of carbon materials reduces overall energy density when employed in large proportions. Therefore, a holistic consideration of these factors is essential when leveraging carbon materials to optimize Li_2S-based LSBs for practical applications.

3.2 Li_2S/metal compounds composite cathode materials

Compared to carbon materials, the electrochemical properties of LSBs can be further enhanced by directly combining metal compounds with Li_2S [78–81]. Firstly, metals possess excellent electrical conductivity. Secondly, metal disulfides and lithium metal can be electrochemically converted into Li_2S and metal elements at low voltages, offering a simple, cost-effective, and uniform *in-situ* synthesis method for Li_2S/metal cathode materials [26, 75–77]. Thirdly, transition metal sulfides can reduce the ion/electron diffusion distances and provide adsorption sites for polysulfides, thus promoting the redox reactions [10, 80, 82–88].

Cui et al. [89] synthesized Li_2S/Co nanocomposites by the *in-situ* conversion of molten lithium with CoS_2 (Fig. 8(a)). The *in-situ* synthesized Li_2S/metal nanocomposites exhibited better environmental stability than pristine Li_2S particles due to protective metal layer on the composite surface, preventing reaction with atmospheric moisture. High-resolution transmission electron microscopy (HRTEM) showed that the Co and Li_2S domains were crystalline with particle sizes of about 5 nm (Fig. 8(b)). When added to the commercial $LiFePO_4$ as a pre-lithium reagent, the nanocomposite could stably cycle for

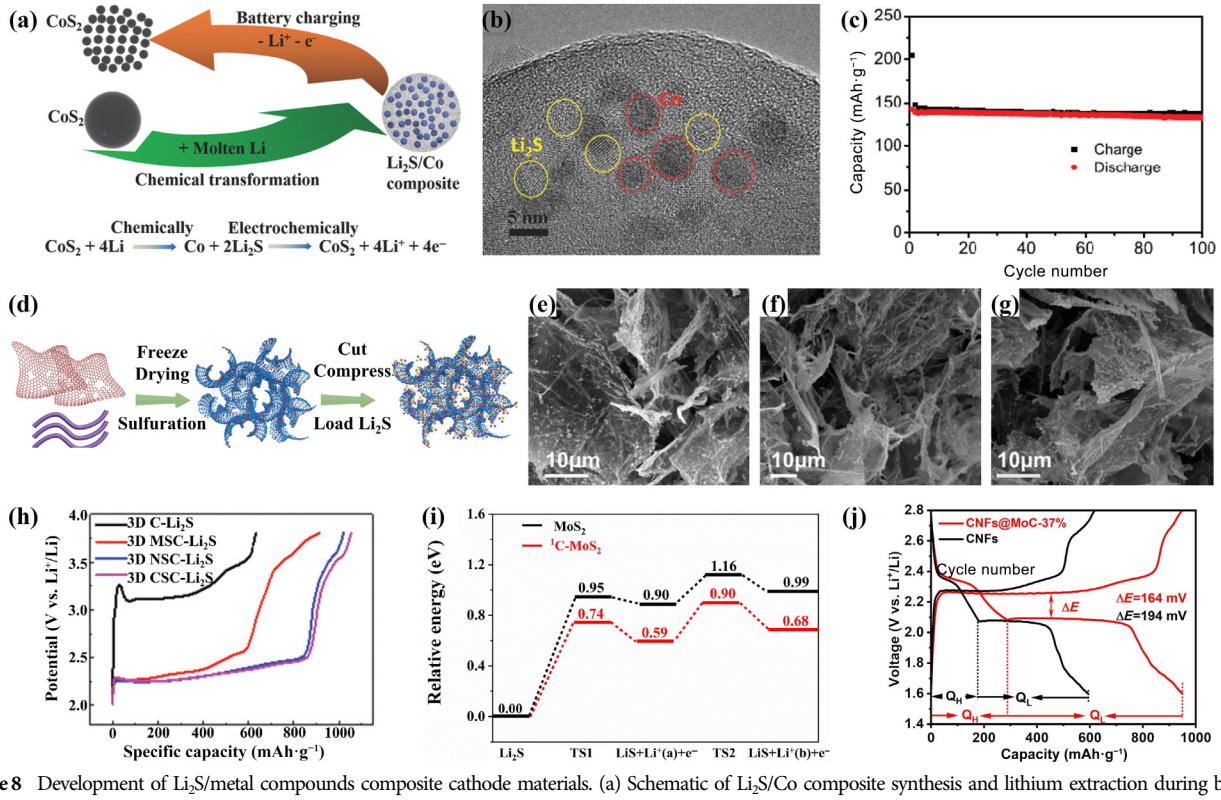

Figure 8 Development of Li_2S/metal compounds composite cathode materials. (a) Schematic of Li_2S/Co composite synthesis and lithium extraction during battery charging. (b) HRTEM images reveal Li_2S/Co nanocomposites with ~ 5 nm Li_2S and Co nanocrystals. (c) Cycling stability of $LiFePO_4$ electrodes with 4.8% Li_2S/Co additive. Reproduced with permission from Ref. [89], © 2016 WILEY-VCH Verlag GmbH & Co. KGaA, Weinheim. (d) Synthesis process of the 3DTSC composite. SEM images of (e) 3DCSC-Li_2S, (f) 3DNSC-Li_2S, and (g) 3DMSC-Li_2S. (h) Initial charge profiles of 3DCSC-Li_2S, 3DNSC-Li_2S, 3DMSC-Li_2S, and 3DC-Li_2S. Reproduced with permission from Ref. [90], © 2019 WILEY-VCH Verlag GmbH & Co. KGaA, Weinheim. (i) Energy profile for the decomposition of Li_2S molecule and Li ion diffusion on pristine MoS_2 and ^{1}C-MoS_2 surfaces. Reproduced with permission from Ref. [91], ©. Elsevier Ltd. 2023. (j) The galvanostatic charge–discharge curves of CNFs@MoC-37 %/Li_2S and CNFs/Li_2S cathode. Reproduced with permission from Ref. [92], © 2025 Elsevier B.V.

150 cycles, indicating no negative effects on the positive electrode material (Fig. 8(c)). The use of metal particles as composites is crucial due to their superior electrical conductivity and catalytic performance. He et al. [90] proposed a 3D transition metal sulfide-decorated carbon sponge (3DTSC) with excellent electrocatalytic and absorption activity, which consists of 0D transition metal sulfide (TS, TS = NiS, CoS, MnS) nanodots, 1D carbon nanowires, and 2D graphene nanosheets (Fig. 8(d)). As shown in Figs. 8(e)–8(g), SEM images revealed an even distribution of Li_2S nanoparticles in the 3DCSC matrix, which is attributed to the abundant mesopores that enable homogeneous Li_2S loading. Figure 8(h) compares the first charge curves of 3DCSC-Li_2S, 3DNSC-Li_2S, 3DMSC-Li_2S, and 3DC-Li_2S electrodes, with 3DTSC-Li_2S showing no significant initial barrier, demonstrating the ability of CoS, NiS, and MnS to reduce the high initial barrier and accelerate the transformation of polysulfides The rate capabilities of these cathodes were evaluated at different charge and discharge rates from 0.1 C to 2 C. Compared with pristine Li_2S, the introduction of metal sulfides accelerates the redox kinetics of polysulfides, thereby delivering exceptional rate capability. Specifically, the 3DCSC-Li_2S cathode achieved a maximum capacity of 492 mAh·g^{-1} at 2 C. When the rate was switched to 0.1 C, the assembled LSB showed the best recovery ability. MoS_2, a prototypical transition metal dichalcogenide, has been widely applied in catalytic systems. Analogous to the carbon-coating strategy, encapsulating Li_2S with carbon-doped MoS_2 outperforms the electrochemical performance achieved by graphene encapsulation.

Theoretical results for one of the doping schemes illustrated in Fig. 8(i) reveal that carbon incorporation enhances Li_2S binding strength, thereby offering a viable route to lower the decomposition barrier during the initial charge [91]. Similarly, Mo-based compounds such as MoC also exhibit excellent catalytic performance. Ji et al. [92] employed electrospinning followed by carbothermal reduction to uniformly anchor MoC nanoparticles onto CNTs, onto which Li_2S was subsequently deposited. Electrochemical measurements reveal that MoC incorporation delivers a higher initial discharge specific capacity and markedly mitigates electrochemical polarization, as shown in Fig. 8(j).

The key advantage of metal compounds lies in their polar surfaces, which chemically adsorb polysulfides to suppress the "shuttle effect" while promoting Li_2S decomposition and thus enhancing reaction kinetics. In some synthesis processes, the heterointerface formed between Li_2S and metal compounds effectively lowers the Li^+ migration barrier. While Li_2S/metal compounds cathodes can improve the electrochemical performance compared to pure Li_2S particles. However, transition metals are not inert during cycling, leading to metal consumption and poor cycle performance, along with electrode polarization [23, 83]. Therefore, further precision engineering of existing composite architectures is imperative to fully unlock the maximal benefits that metal compounds can deliver to LSBs systems.

3.3 Li_2S/conductive polymer composite cathode materials

Conductive polymers offer a significant alternative to carbon and metal materials when combined with Li_2S, leveraging their distinct advantages. Notably, conductive polymers possess excellent mechanical properties that enhance the structural stability and accommodate volume changes during continuous cycles [22]. Their customizable nature ensures good contact with the active material, crucial for maintaining electrode stability. Moreover, these polymers exhibit good electrical conductivity, which can significantly improve the electron conductivity of the composite material and enhance the diffusion rates in the electrode materials [84, 85]. Similar to the polar surfaces of metal compounds, the functional groups of the polymers can effectively absorb polysulfides, inhibiting "shuttle effect" and enhancing cycling performance [20, 86]. Although extensive research exists on sulfur cathodes, studies on Li_2S/conductive polymer composites are less common. Seh et al. [93] *in-situ* synthesized Li_2S-polypyrrole (Li_2S-PPy) composites by mixing Li_2S and PPy (Fig. 9(a)). High-resolution XPS analysis revealed strong Li-N interactions within the polypyrrole, confining polysulfides in the polymer matrix during cycling. In addition, the conductivity of PPy ensures close contact with Li_2S, providing an efficient electronic channel and

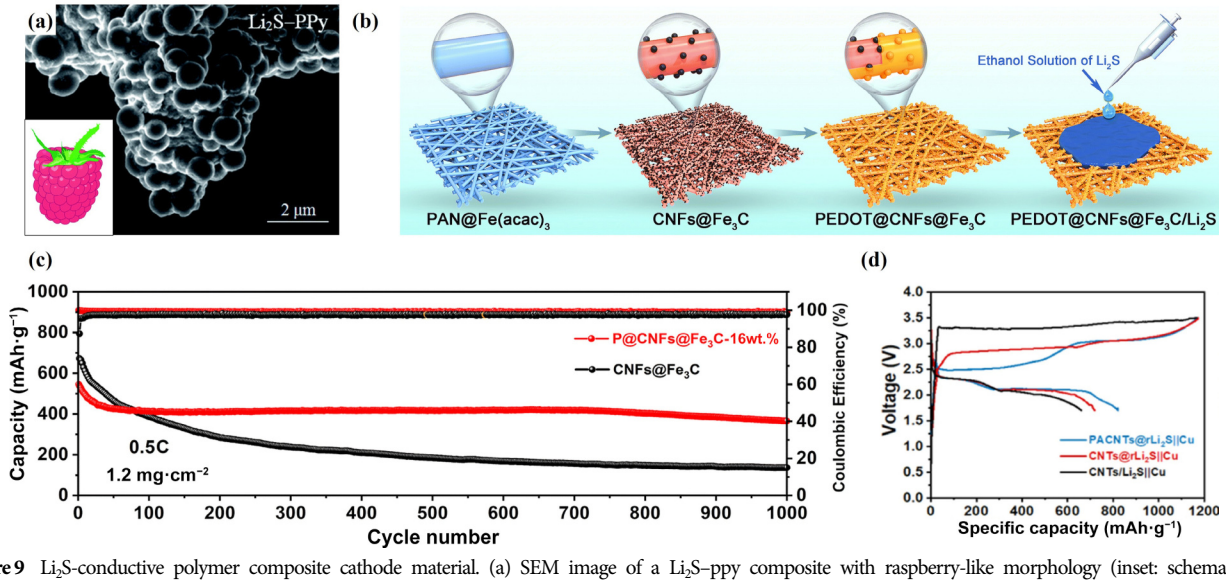

Figure 9 Li_2S-conductive polymer composite cathode material. (a) SEM image of a Li_2S–ppy composite with raspberry-like morphology (inset: schematic of raspberry-like structure). Reproduced with permission from Ref. [93], © 2014 The Royal Society of Chemistry. (b) Synthesis process of the PEDOT@CNFs@Fe_3C/Li_2S composite cathode. (c) The P@CNFs@Fe_3C-16 wt.%/Li_2S cathode exhibits a 0.033% capacity decay per cycle at 0.5C. Reproduced with permission from Ref. [94], © 2025 The Royal Society of Chemistry. (d) Charge and discharge curves of PACNTs@rLi_2SCu AFLSB at the 1st cycle. Reproduced with permission from Ref. [95], © 2025 Elsevier B.V.

improving the reaction kinetics. The Li_2S-PPy composite cathode demonstrated stable cycling performance at 0.2 C, with an initial capacity of 785 $mAh·g^{-1}$. The capacity retention values achieved at the end of 50, 100, and 200 cycles were 91%, 91%, and 84%, respectively, relative to the initial cycle. Recently, Yang et al. [94] designed a novel Li_2S host architecture in which Fe_3C nanoparticles and CNFs are intimately bridged by poly(3,4-ethylenedioxythiophene) (PEDOT) coating, yielding a highly conductive 3D network, as shown in Fig. 9(b). This study reveals that PEDOT plays a significant role in both adsorbing and converting polysulfides. An optimized PEDOT loading endows the composite cathodes with exceptional cycling stability (Fig. 9(c)), delivering a 67% capacity retention after 1000 cycles at 0.5 C, corresponding to a minimal decay of only 0.033% per cycle. Employing polymer-functionalized CNTs as a host, Li_2S can also be generated *in-situ* via the reaction between S and Li_3N within this architecture [95]. Poly(1-aminoanthraquinone) (PAAQ) acts as a redox mediator in the cathode, enhancing the electrochemical activity of Li_2S and yielding both a lower activation barrier and a reduced voltage plateau during the initial charge process (Fig. 9(d)). Even at an ultrahigh Li_2S loading of 15.2 $mg·cm^{-2}$, the assembled anode-free LSB retains an areal specific capacity of ~ 5.4 $mAh·cm^{-2}$ after 200 cycles.

Conductive polymers lower the Li_2S activation barrier through three intrinsic advantages: (I) their chain-like architecture intimately encapsulates Li_2S together with other components, simultaneously minimizing interfacial resistance and buffering contact loss caused by volume expansion; (II) specific functional groups can form stable chemical bonds with Li_2S, facilitating Li–S bond cleavage during activation; and (III) selected polymers function as RMs within the cathodes, accelerating Li_2S conversion. Nevertheless, polymer degradation or structural collapse during prolonged cycling necessitates the integration of polymers with carbon materials to construct hierarchical host architectures.

4 Electrolyte engineering

Electrolyte selection is critical in LSBs research, with ether-based electrolytes being widely preferred because of the high ionic conductivity, low viscosity, and electrochemical stability to polysulfides and sulfur radicals [88, 96]. The combination of dioxolane (DOL) and dimethoxyethane (DME) often outperforms individual solvents or other options, as DME's higher ionic conductivity improves the reaction kinetics, and DOL's ability to form solid electrolyte interface (SEI) on the lithium anodes alleviates the shuttle effect [90, 96]. Lithium bistrifluoromethionate (LiTFSI) is commonly selected as the lithium salt due to its temperature stability, optimal number of donors, high ionic conductivity, and low viscosity in ether-based solvents [91, 92]. In addition, $LiNO_3$ contributes to SEI film formation on the surface of lithium metal anode, protecting the anode, reducing polysulfide shuttling, and even aiding in the deposition of lithium metal [97–99]. While ether-based electrolytes dominate, a minority of studies explore ester-based electrolytes [26, 93, 100]. However, the lithium polysulfides formed during cycling may react with carbonates such as polypropylene carbonate (PC), vinyl carbonate (EC), and diethyl carbonate (DEC), which adversely affects the electrochemical performance, rendering the ester-based electrolytes incompatible with the LSBs battery system [101, 97]. Although the DOL/DME electrolytes containing 1 M LiTFSI and 2 wt.% $LiNO_3$ possess a high initial discharge capacity, the issues such as polysulfide dissolution, shuttle effect, and lithium anode corrosion persist, preventing the achievement of satisfactory cycling performance [102]. The significant issue of the high initial activation barrier of Li_2S also remains unresolved. Hence, suitable electrolytes for the Li_2S battery systems still need to be developed.

4.1 Electrolyte additives

It has been reported that the activation of Li_2S cathode materials is closely associated with the complementary nucleation of Li_2S in polysulfides, and the addition of polysulfides in the electrolyte has been shown to facilitate the activation of Li_2S [30]. Currently, polysulfides seem to be a favorable solution to the Li_2S activation issue. In fact, many researchers have begun to utilize polysulfides not just as additives but as cathode electrolytes, making a new tendency in Li_2S research. This section thus reviews the notable examples of lithium polysulfide cathode electrolytes and redox media that can be employed as alternative activators for polysulfides.

By adding P_2S_5 to the electrolyte, Zu et al. [29] successfully integrated commercially available bulk Li_2S particles into cathodes. Electrochemical results showed that these particles were effectively activated without high charging cutoff voltages. The interaction between P_2S_5 and Li_2S was found to decrease battery resistance, improve interface stability and enhance the oxidation of Li_2S to the polysulfide surface, significantly reducing the initial charging voltage plateau. This suggests that Li_2S was effectively oxidized to polysulfide, with the activation process involving the formation of intermediate sulfur and phosphorus-containing substances on the surface of Li_2S, which can serve as active sites to promote surface charge transfer and oxidation of Li_2S. The P_2S_5-activated Li_2S achieved a reversible discharge capacity of 800 $mAh·g^{-1}$ at C/10 with an 83% capacity retention rate after 80 cycles and a coulombic efficiency close to 100% throughout the cycles. Beyond polysulfide electrolyte additives, Yang et al. [103] assembled a novel lithium/polysulfide (Li/PS) semi-liquid battery for large-scale energy storage, using lithium polysulfide (Li_2S_8) in ether solvent as the cathode and lithium metal as the anode (Fig. 10(a)). The cathode of this semi-liquid battery operates solely between sulfur and Li_2S_4, avoiding the formation and volume expansion of solid Li_2S_2/Li_2S, and holds potential for the development of a liquid battery system (Fig. 10(b)). In addition, the battery system includes $LiNO_3$ as an additive, forming a stable passivation layer on the surface of the metal lithium anode. At the same time, the passivation layer can also act as a SEI to prevent adverse reactions and internal shuttle effect, forming stable reaction interface and allowing the polysulfide cathode to directly contact the lithium anode without reaction. This novel design enables film-free liquid battery with a good cycle life. When 5 M of polysulfide solution is used on the cathode side, the energy density can reach 149 $Wh·L^{-1}$ (133 $Wh·kg^{-1}$), which is about five times that of a vanadium redox battery (Fig. 10(c)). Compared to traditional solid electrodes, the aqueous solution LSBs offer the advantage of high solubility of Li_2S_4/Li_2S redox in the cathode, thus promoting the redox reactions [104], the all-liquid electrodes and reactions provide rapid surface reaction and negligible volume expansion. These water-based LSBs provide a new perspective for the development of large-scale energy storage in the future.

RMs serve as an alternative to polysulfide cathode electrolytes, facilitating continuous redox reactions that cycle substances between the active material and the electrode surface without the need for physical contact [105, 106]. Fig. 10(d) illustrates how RMs function. RMs can undergo electrooxidation on the electrode surface (RM to RM^+), diffuse into the active materials, oxidize the

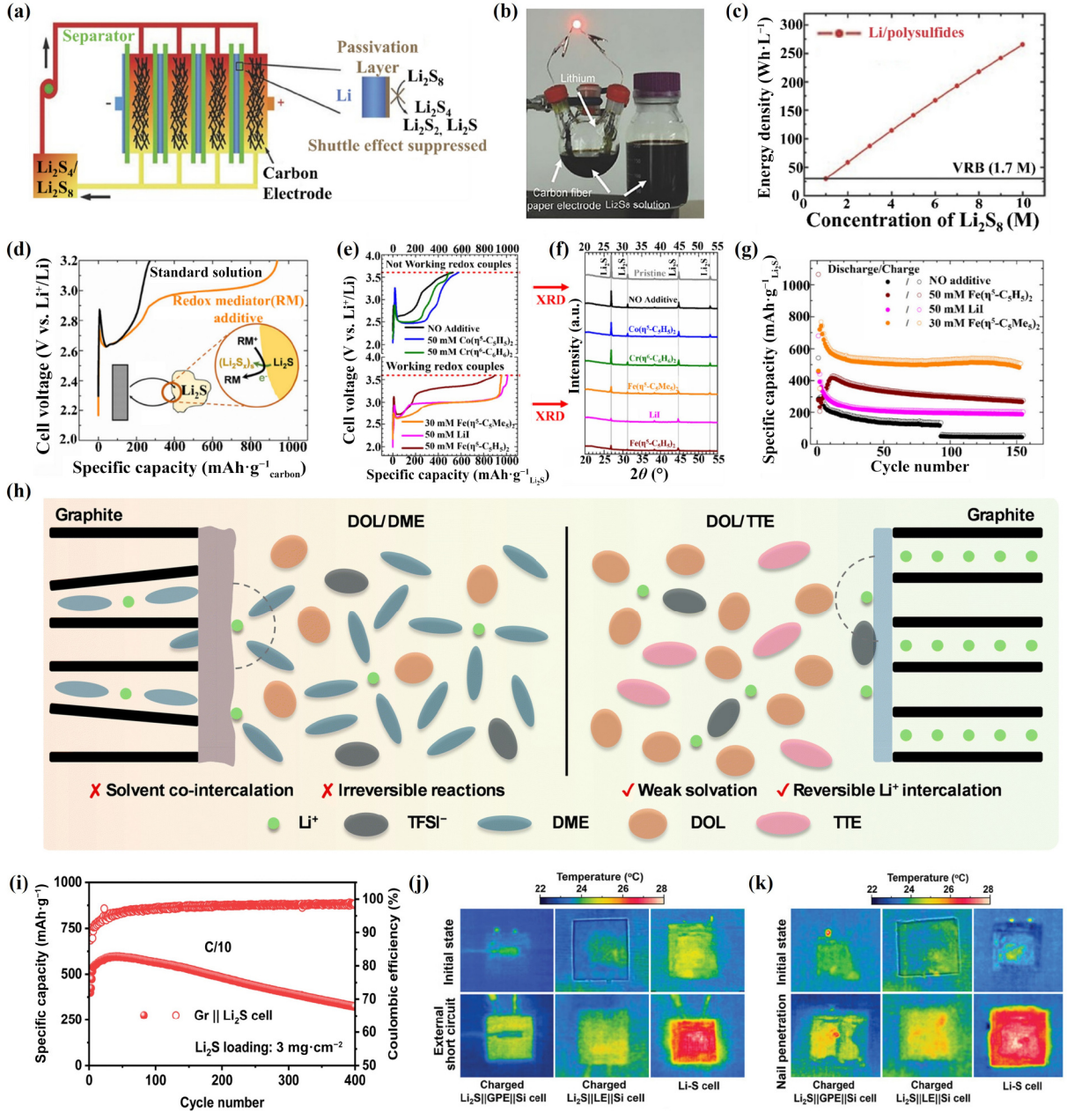

Figure 10 Electrolyte engineering for enhancing the performance of Li_2S cathode. (a) Schematic of lithium-polysulfide flow battery configuration. Enlarged view demonstrates $LiNO_3$-induced passivation layer effectively inhibits Li/polysulfide side reactions, significantly reducing shuttle effect. (b) Membrane-free cell performance using Li anode and carbon fiber cathode in Li_2S_8 catholyte. (c) Volumetric energy density vs. sulfur concentration, with vanadium flow battery reference. Reproduced with permission from Ref. [103], © 2013 The Royal Society of Chemistry. (d) RMs operation mechanism. (e) Charging profiles and (f) XRD patterns of Li_2S electrodes (233 mA·g^{-1} to 3.6 V_{Li}) with baseline electrolyte (10% LiTFSI + 2% $LiNO_3$ in DME/DOL 1:1) vs. additives: $CoCp_2$, dibenzenechromium, LiI, $FeCp_2$, decamethylferrocene. (g) Cycling stability of Li/Li_2S cells with baseline vs. mediator-enhanced electrolytes (LiI, $FeCp_2$, decamethylferrocene), charged at C/10 (0.5 mA) to specified voltages then cycled 1.9–2.6 V_{Li}. Reproduced with permission from Ref. [107], © 2014 American Chemical Society. (h) Schematic showing the solvation structure and intercalation behaviors of the DOL/DME and DOL/TTE electrolytes with Gr anodes. (i) Cycling performance of Gr Li_2S full cell in DOL/TTE electrolyte. Reproduced with permission from Ref. [111], © 2025 The Royal Society of Chemistry. Infrared thermography of charged Li_2S@M-PANGPESi, Li_2S@M-PANLESi and Li–S cell after external short circuit (j) and nail penetration (k). Reproduced with permission from Ref. [112], © 2022 Wiley-VCH GmbH.

active substance (RM^+ to RM), and then return to the electrode surface for recycling. In this reversible process, RMs significantly enhances the transfer of electrons from the active substance to the electrode. Five additives have been reported by Meini et al. [107] and the additives tested in this study contain all three possibilities: $E_{RM} < E_{Li_2S}$ (cobaltous cene), $E_{RM} \approx E_{Li_2S}$ (diphenyl chromium), and $E_{RM} > E_{Li_2S}$ (decamethylferrocene, LiI, and ferrocene). The third category was expected to act as RMs because of the voltage difference providing a high driving force compared to E_{Li_2S}. To demonstrate this concept, charging experiments were performed with the Li_2S electrode at a relatively high C/5 ratio, and the cathode was analyzed by XRD after charging to 3.6 V_{Li} to detect any residual Li_2S (Fig. 10(e)). XRD analysis showed that ferrocene, LiI, and decamethylferrocene left negligible Li_2S in the cathode matrix after oxidation to 3.6 V_{Li}, indicating effective utilization of the active material (Fig. 10(f)). The results of C/10 charging-discharging cycles showed that decamethylferrocene enabled outstanding Li_2S utilization at a low charging potential of 3.2 V.

Even after extended cycling Li/Li_2S batteries containing this additive maintained a stable capacity value of about 490 mAh·g^{-1}, four times higher than those with standard electrolytes without additives (Fig. 10(g)). These findings suggest that activating Li/Li_2S cells at lower potentials improve capacity retention, achievable with appropriate RMs. RMs, like InI_3 and some quinone derivatives, can alleviate the activation barrier of the Li_2S cathode, thereby increasing the initial specific capacity and improving the cycling and rate performance [94, 95]. InI_3, for instance, forms a passivation layer on the cathode and anode, which can form a stable interface, inhibiting the "shuttle effect" and protecting the electrodes, thereby improving the electrochemical performance of the battery. It is found that using RMs additive to address the initial activation barrier of Li_2S cathode is a promising approach, as they enhance the electron transfer to the surface of Li_2S material, improve the conductivity of the material, and form passivation layers that protect the electrodes and mitigate the "shuttle effect", thus improving the overall electrochemical performance [22].

4.2 Solute-solvent optimization

Conventional electrolytes are generally prepared by dissolving a prescribed amount of electrolyte salt in a solvent. Therefore, beyond introducing additives into existing electrolytes, optimizing both solute and solvent offers an alternative route to enhance Li_2S-based LSB performance [108, 109].

Regarding the solute, the lithium salt serves as a critical Li^+ source during cycling. In high-concentration electrolytes (HCEs), salt concentrations exceed 3 M, and the scarcity of free solvent molecules markedly decreases polysulfide solubility, thereby mitigating the "shuttle effect". In the study of Li_2S/graphene composites, the authors demonstrated the effect of the molar concentration of the electrolyte salt on the specific capacity and stability of the produced cathode [63]. The discharge capacity with 5 and 7 M electrolytes at C/10 is higher than that of 3 M. While in the 1 M electrolyte, the capacity rapidly drops to less than 25% of the initial capacity after 50 cycles, which may be due to active cathode material loss from polysulfide dissolution and the increased resistance. Therefore, increasing the salt concentration in the electrolyte significantly improve the cycling stability by improving interface stability. However, the elevated salt concentration in HCEs increases viscosity and decreases ionic conductivity, inducing pronounced polarization. Consequently, the higher charge overpotential in the initial cycle further raises the activation barrier, significantly degrading electrochemical performance, especially at high rates. On this basis, introducing an inert diluent to prepare localized high-concentration electrolytes (LHCEs) has emerged as a pivotal solute-solvent optimization strategy. This approach preserves the solvation structure of HCEs while leveraging the advantages of high salt activity and low viscosity.

An ideal diluent is an additive that neither engages in Li^+ solvation nor alters the primary solvation sheath, serving solely to reduce electrolyte viscosity and cost. Fluorinated ethers, as the most common diluent, have been widely used in LHCEs. A study has demonstrated that the SEI formed in both HCE and LHCE systems is rich in fluorine composition and relatively poor in oxygen composition, yielding enhanced interfacial stability. In particular, LHCEs obtained by diluting HCEs with a non-coordinating hydrofluoroether (HFE) solvent exhibit markedly lower polysulfide solubility [110]. Recently, Lai et al. [111] replaced DME with 1,1,2,2-tetrafluoroethyl-2,2,3,3-tetrafluoropropylether (TTE) to obtain an optimized ether-based electrolyte (1 M LiTFSI in DOL/TTE). Unlike DME-based electrolyte, the TTE-based electrolyte suppresses solvent co-intercalation and reductive decomposition, thereby markedly enhancing the stability of graphite anode (Fig. 10(h)). The assembled graphite//Li_2S full cell exhibits stable overpotentials and specific capacities over 100 cycles, retaining a reversible capacity of 257 mAh·g^{-1} even after 400 cycles (Fig. 10(i)). Although TTE is employed here in a manner distinct from its role in conventional LHCEs, the results underscore the exceptional capacity of fluorinated ethers to suppress polysulfide dissolution and enhance interfacial stability. Consequently, their function within LHCEs remains pivotal. In the future, the development of cost-effective fluorinated ether diluents promises to accelerate the commercial deployment of LHCEs in Li_2S-based LSBs and lithium metal batteries. It should be noted, however, that excessive fluorination can raise the organic content of the SEI, potentially increasing interfacial impedance.

4.3 Solid or hybrid liquid-solid electrolytes

In addition to high performance, practical battery systems must prioritize safety and convenience. Conventional liquid electrolytes have proven highly compatible with LSBs and are already widely deployed. Yet, as advanced applications impose increasingly stringent demands on energy storage devices, quasi-solid and all-solid batteries have emerged as next-generation solutions.

Gel polymer electrolytes (GPEs) are quasi-solid electrolytes formed by absorbing liquid electrolytes into a polymer matrix, offering both robust mechanical strength and efficient ionic transport. Meng et al. [112] designed a novel GPE based on $Ti_3C_2T_x$ MXene, poly(vinylidene fluoride-co-hexafluoropropylene) (PVDF-HFP), and mixed ether-carbonate electrolyte that is compatible with both Li_2S cathode and Si anode. The assembled quasi-solid-state full cell delivers a maximum energy density of 1108 Wh·kg^{-1} and a maximum power density of 5063 kW·kg^{-1}, demonstrating exceptional practical potential. As shown in Figs. 10(j) and 10(k), the full cell exhibits only a minor temperature rise after external short-circuit or nail-penetration tests, confirming the superior safety of the developed GPE. Polyethylene oxide (PEO) [113] and long-chain polymers [114] formed by 1T-MoS_2-induced ring-opening polymerization of DOL are also employed as polymer matrices for GPEs. In these quasi-solid electrolytes, the polymer network acts as a physical barrier that suppresses polysulfide shuttling while eliminating the leakage risks associated with liquid electrolytes, thus laying the groundwork for practical, metal-free LSBs—especially those utilizing Li_2S cathodes.

Because GPEs fall short of liquid electrolytes in ionic conductivity, hybrid solid-liquid electrolytes (HSLEs) have emerged as an alternative optimization strategy. By incorporating a small fraction of liquid electrolyte into a solid-state matrix, these hybrids create solid-liquid synergistic interfaces that deliver ionic conductivities comparable to those of liquid electrolytes, thereby enabling high-rate performance. Dissolving LiTFSI salt in acetonitrile (MeCN) with 1,1,2,2-tetrafluoroethyl 2,2,3,3-tetrafluoropropyl ether (TTE) cosolvent and applying the resulting interlayer material onto the surface of $Li_7P_3S_{11}$ solid electrolyte yields a high-performance HSLE [115]. Compared with the pristine solid-state electrolyte, the incorporation of the liquid phase yields a pronounced performance boost: reversible capacity rises from 330 to 760 mAh·g^{-1} after 100 cycles. Electrochemical impedance spectroscopy further reveals that the interlayer

progressively reduces interfacial resistance as cycling proceeds. These enhancements stem from improved electrolyte-Li_2S contact enabled by the wetting action of the liquid component. While the solid electrolyte provides a rigid framework, the liquid phase supplies continuous ionic pathways; their synergistic interplay lowers the Li_2S activation barrier and enables high-rate capability, providing potential for advanced HSLEs.

5 Summary and perspectives

This review summarizes the key strategies for addressing Li_2S cathode challenges, mainly includes: (I) composite material engineering by integrating Li_2S with carbon matrices, metal sulfides, or conductive polymers; (II) electrolyte optimization favoring ether-based systems with polysulfide/RM additives over ester alternatives to mitigate side reactions; (III) developing next-generation solid or hybrid liquid-solid electrolytes brings LSBs closer to practical standard, opening new avenues toward high-performance Li_2S-based systems. Crucial advancements focus on synergizing conductivity, catalytic activity and interfacial stability.

Despite these progresses, the electrochemical process mechanism of Li_2S cathodes is not well understood, and there is vast room for advancement in the practical and commercial application of Li_2S cathode and the improvement of full batteries. Future perspectives on Li_2S cathode development include the following aspects (Fig. 11).

(I) Compatibility with lithium-free anodes:

A key advantage of Li_2S over commercial sulfur is its intrinsic lithium content; eliminating metallic lithium not only enhances safety but also lowers production costs. In future, more efforts could be devoted to the following aspects:

a. Investigating Li_2S pairing with graphite, silicon, or tin anodes to enable lithium-free LSBs.

b. Addressing challenges like poor anode conductivity and volume expansion through advanced electrode engineering (e.g., prelithiation, nanostructuring).

(II) Cost-effective synthesis methods:

Developing scalable, air-stable Li_2S synthesis routes to reduce reliance on inert-atmosphere processing and lower production costs.

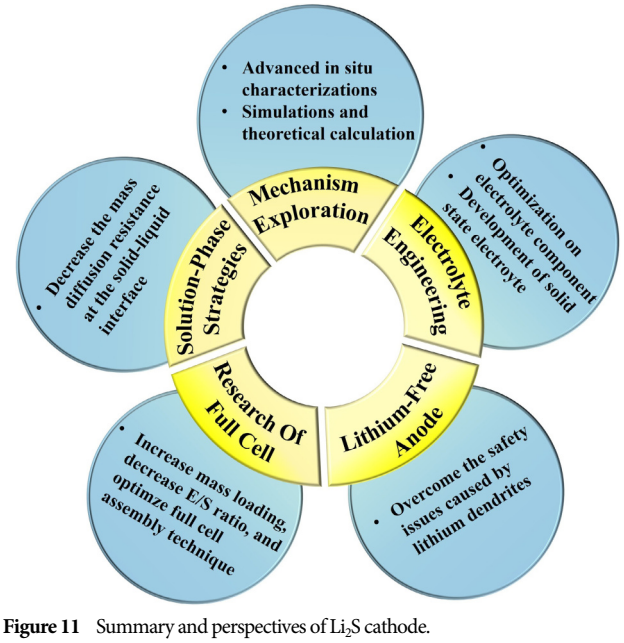

Figure 11 Summary and perspectives of Li_2S cathode.

(III) Elucidation of Li_2S activation mechanism:

a. Conducting fundamental studies (e.g., *in-situ* spectroscopy, computational modeling) to resolve controversies over the high activation barrier during initial charging.

b. Using mechanistic insights to guide cathode design (e.g., defect engineering, catalytic interfaces).

(IV) Advanced electrolyte engineering:

As a vital component of any battery system, the electrolyte directly governs safety, cost, and scalability. Advanced electrolyte designs can lower the initial activation barrier of Li_2S, circumventing the need for overly complex electrode architectures and paving the way for scalable manufacturing. Moreover, solid or quasi-solid electrolytes are better suited for practical applications such as wearable electronics. Future efforts should be devoted to the following two parts.

a. Optimizing ether-based electrolytes by tailoring solvents, lithium salts, and RMs to enhance Li_2S redox kinetics and stability.

b. Exploring solid-state or hybrid electrolytes to mitigate polysulfide shuttling and interfacial degradation.

(V) Li_2S solution-phase strategies:

Solution-based design involves every stage of battery development—from material synthesis to battery performance.

a. Decreasing mass diffusion resistance at the liquid-solid interface, thus improving reaction kinetics and reducing activation barriers.

b. Simplifying solvent purification processes and identify low-cost, high-stability solvents (e.g., tailored ethers, ionic liquids).

(VI) Full cell integration and scalability:

Pouch-cell performance serves as a critical reference for translating coin-cell results to practical applications. Therefore, when considering larger scale applications, a comprehensive evaluation encompassing safety, cost, sustainability, and overall performance must be systematically integrated.

a. Progressing from lab-scale half-cells to practical full-cell configurations with high Li_2S loading and low electrolyte-to-sulfur (E/S) ratios.

b. Validating long-term cycling stability, safety, and energy density for commercial viability.

Despite the considerable challenges, we remain confident that with collaborative research efforts, the practical application of LSBs with Li_2S cathodes will be realized soon.

Acknowledgements

This work was supported by the National Key R&D Program (Grant No.: 2022YFA1504100), the Natural Science Foundation of China (Grant No.: 52372170, 52301296, 52261160573), Hebei Provincial Department of Science and Technology-Basic Research Cooperation Project of Beijing-Tianjin-Hebei Region (B2024204027), the Beijing Natural Science Foundation (Z230019), the Institute of Process Engineering (IPE) Project for Frontier Basic Research, Grant No. QYJC-2022-008.

Declaration of conflicting interests

The authors declare no conflicting interests regarding the content of this article.

Data availability

All data needed to support the conclusions in the paper are presented in the manuscript. Additional data related to this paper may be requested from the corresponding author upon request.

References

[1] Zhang, D.; Luo, Y. X.; Wu, B.; Zeng, P.; Xiang, C.; Zhao, C. K.; Sofer, Z.; Chen, M. F.; Wang, X. Y. A heterogeneous FeP–CoP electrocatalyst for expediting sulfur redox in high-specific-energy lithium–sulfur batteries. *Electrochim. Acta* **2021**, *397*, 139275.

[2] Zhao, C.; Xu, G. L.; Yu, Z.; Zhang, L. C.; Hwang, I.; Mo, Y. X.; Ren, Y. X.; Cheng, L.; Sun, C. J.; Ren, Y. et al. A high-energy and long-cycling lithium–sulfur pouch cell via a macroporous catalytic cathode with double-end binding sites. *Nat. Nanotechnol.* **2021**, *16*, 166–173.

[3] Yang, R. L.; Chen, Y.; Pan, Y. X.; Kim, M.; Liu, H.; Lee, C. K. W.; Huang, Y. Y.; Tang, A. D.; Tu, F. Y.; Li, T. B. et al. Single-step laser-printed integrated sulfur cathode toward high-performance lithium–sulfur batteries. *Nat. Commun.* **2025**, *16*, 2386.

[4] Wang, H. B.; Liu, J.; Ju, W. Q.; Xu, X. P.; Chen, J. W. Nitrogen-doped hollow carbon sphere composite Mn_3O_4 as an advanced host for lithium–sulfur battery. *Sci. Rep.* **2024**, *14*, 13714.

[5] Xu, W. X.; Lang, S. Y.; Wang, K. Y.; Zeng, R.; Li, H. Q.; Feng, X. R.; Krumov, M. R.; Bak, S. M.; Pollock, C. J.; Yeo, J. J. et al. Fundamental mechanistic insights into the catalytic reactions of Li–S redox by Co single-atom electrocatalysts via *operando* methods. *Sci. Adv.* **2023**, *9*, eadi5108.

[6] Cai, K. P.; Song, M. K.; Cairns, E. J.; Zhang, Y. G. Nanostructured Li_2S–C composites as cathode material for high-energy lithium/sulfur batteries. *Nano Lett.* **2012**, *12*, 6474–6479.

[7] Wang, D. W.; Zeng, Q. C.; Zhou, G. M.; Yin, L. C.; Li, F.; Cheng, H. M.; Gentle, I. R.; Lu, G. Q. M. Carbon–sulfur composites for Li–S batteries: Status and prospects. *J. Mater. Chem. A* **2013**, *1*, 9382–9394.

[8] Yin, Y. X.; Xin, S.; Guo, Y. G.; Wan, L. J. Lithium–sulfur batteries: Electrochemistry, materials, and prospects. *Angew. Chem., Int. Ed.* **2013**, *52*, 13186–13200.

[9] Liu, Y. Z.; Meng, X. Y.; Wang, Z. Y.; Qiu, J. S. A Li_2S-based all-solid-state battery with high energy and superior safety. *Sci. Adv.* **2022**, *8*, eabl8390.

[10] Li, S. Q.; Leng, D.; Li, W. Y.; Qie, L.; Dong, Z. H.; Cheng, Z. Q.; Fan, Z. Y. Recent progress in developing Li_2S cathodes for Li–S batteries. *Energy Storage Mater.* **2020**, *27*, 279–296.

[11] Li, Z.; Zhang, S. G.; Zhang, C.; Ueno, K.; Yasuda, T.; Tatara, R.; Dokko, K.; Watanabe, M. One-pot pyrolysis of lithium sulfate and graphene nanoplatelet aggregates: *In situ* formed Li_2S/graphene composite for lithium–sulfur batteries. *Nanoscale* **2015**, *7*, 14385–14392.

[12] Yang, H. L.; Lei, Y. J.; Yang, Q. R.; Zhang, B. W.; Gu, Q. F.; Wang, Y. X.; Chou, S. L.; Liu, H. K.; Dou, S. X. Cobalt-induced highly-electroactive Li_2S heterostructured cathode for Li–S batteries. *Electrochim. Acta* **2023**, *439*, 141652.

[13] Hassoun, J.; Scrosati, B. A high-performance polymer tin sulfur lithium ion battery. *Angew. Chem., Int. Ed.* **2010**, *49*, 2371–2374.

[14] Yang, Y.; McDowell, M. T.; Jackson, A.; Cha, J. J.; Hong, S. S.; Cui, Y. New nanostructured Li_2S/silicon rechargeable battery with high specific energy. *Nano Lett.* **2010**, *10*, 1486–1491.

[15] Kong, L. L.; Wang, L.; Ni, Z. C.; Liu, S.; Li, G. R.; Gao, X. P. Lithium–magnesium alloy as a stable anode for lithium–sulfur battery. *Adv. Funct. Mater.* **2019**, *29*, 1808756.

[16] Wei, P.; Wang, H. Y.; Yang, M.; Wang, J. Y.; Wang, D. Relocatable hollow multishelled structure-based membrane enables dendrite-free lithium deposition for ultrastable lithium metal batteries. *Adv. Energy Mater.* **2024**, *14*, 2400108.

[17] Wang, H. Y.; Wei, P.; Wang, J. Y.; Wang, D. Hollow multishelled structure reviving lithium metal anode for high-energy-density batteries. *Chem. Res. Chin. Univ.* **2024**, *40*, 428–436.

[18] Lorger, S.; Narita, K.; Usiskin, R.; Maier, J. Enhanced ion transport in Li_2O and Li_2S films. *Chem. Commun.* **2021**, *57*, 6503–6506.

[19] Su, D. W.; Zhou, D.; Wang, C. Y.; Wang, G. X. Toward high performance lithium–sulfur batteries based on Li_2S cathodes and beyond: Status, challenges, and perspectives. *Adv. Funct. Mater.* **2018**, *28*, 1800154.

[20] Castillo, J.; Qiao, L. X.; Santiago, A.; Judez, X.; Buruaga, A. S. D.; Martin, G. J.; Armand, M.; Zhang, H.; Li, C. M. Perspective of polymer-based solid-state Li–S batteries. *Energy Mater.* **2022**, *2*, 200003.

[21] Kim, J. T.; Rao, A.; Nie, H. Y.; Hu, Y.; Li, W. H.; Zhao, F. P.; Deng, S. X.; Hao, X. G.; Fu, J. M.; Luo, J. et al. Manipulating Li_2S_2/Li_2S mixed discharge products of all-solid-state lithium sulfur batteries for improved cycle life. *Nat. Commun.* **2023**, *14*, 6404.

[22] Jiang, J. C.; Fan, Q. N.; Chou, S. L.; Guo, Z. P.; Konstantinov, K.; Liu, H. K.; Wang, J. Z. Li_2S-based Li-ion sulfur batteries: Progress and prospects. *Small* **2021**, *17*, 1903934.

[23] Son, Y.; Lee, J. S.; Son, Y.; Jang, J. H.; Cho, J. Recent advances in lithium sulfide cathode materials and their use in lithium sulfur batteries. *Adv. Energy Mater.* **2015**, *5*, 1500110.

[24] Zalka, D.; Vizintin, A.; Maximenko, A.; Pászti, Z.; Dankházi, Z.; Hegedüs, K.; Shankar, L. S.; Kun, R.; Saksl, K.; Fedorková, A. S. et al. Improving lithium–sulfur battery performance using a polysaccharide binder derived from red algae. *Commun. Mater.* **2025**, *6*, 17.

[25] Kaiser, M. R.; Han, Z. J.; Liang, J.; Dou, S. X.; Wang, J. Z. Lithium sulfide-based cathode for lithium-ion/sulfur battery: Recent progress and challenges. *Energy Storage Mater.* **2019**, *19*, 1–15.

[26] Obrovac, M. N.; Dahn, J. R. Electrochemically active lithia/metal and lithium sulfide/metal composites. *Electrochem. Solid-State Lett.* **2002**, *5*, A70–A73.

[27] Yuan, H. D.; Chen, X. L.; Zhou, G. M.; Zhang, W. K.; Luo, J. M.; Huang, H.; Gan, Y. P.; Liang, C.; Xia, Y.; Zhang, J. et al. Efficient activation of Li_2S by transition metal phosphides nanoparticles for highly stable lithium–sulfur batteries. *ACS Energy Lett.* **2017**, *2*, 1711–1719.

[28] Shi, P. C.; Liang, X.; Xu, K.; Sun, Y.; Cheng, S.; Chen, C. H.; Xiang, H. F. Sulfone-assisted-NH_4I as electrolyte additive with synergistic dissolution and catalysis effects on reducing the activation voltage of Li_2S cathode. *Chem. Eng. J.* **2020**, *398*, 125608.

[29] Zu, C. X.; Klein, M.; Manthiram, A. Activated Li_2S as a high-performance cathode for rechargeable lithium–sulfur batteries. *J. Phys. Chem. Lett.* **2014**, *5*, 3986–3991.

[30] Yang, Y.; Zheng, G. Y.; Misra, S.; Nelson, J.; Toney, M. F.; Cui, Y. High-capacity micrometer-sized Li_2S particles as cathode materials for advanced rechargeable lithium-ion batteries. *J. Am. Chem. Soc.* **2012**, *134*, 15387–15394.

[31] Tan, G. Q.; Xu, R.; Xing, Z. Y.; Yuan, Y. F.; Lu, J.; Wen, J. G.; Liu, C.; Ma, L.; Zhan, C.; Liu, Q. et al. Burning lithium in CS_2 for high-performing compact Li_2S-graphene nanocapsules for Li–S batteries. *Nat. Energy* **2017**, *2*, 17090.

[32] Zhang, K.; Wang, L. J.; Hu, Z.; Cheng, F. Y.; Chen, J. Ultrasmall Li_2S nanoparticles anchored in graphene nanosheets for high-energy lithium-ion batteries. *Sci. Rep.* **2014**, *4*, 6467.

[33] Ren, Y.; Fan, J. S.; Fu, Y. Z. Recent strategies for improving the performances of rechargeable lithium batteries with sulfur- and oxygen-based conversion cathodes. *Energy Mater.* **2023**, *3*, 300015.

[34] Fang, R. P.; Chen, K.; Yin, L. C.; Sun, Z. H.; Li, F.; Cheng, H. M. The regulating role of carbon nanotubes and graphene in lithium-ion and lithium–sulfur batteries. *Adv. Mater.* **2019**, *31*, 1800863.

[35] Seh, Z. W.; Zhang, Q. F.; Li, W. Y.; Zheng, G. Y.; Yao, H. B.; Cui, Y. Stable cycling of lithium sulfide cathodes through strong affinity with a bifunctional binder. *Chem. Sci.* **2013**, *4*, 3673–3677.

[36] Chen, C. G.; Li, D. J.; Gao, L.; Harks, P. P. R. M. L.; Eichel, R. A.; Notten, P. H. L. Carbon-coated core-shell Li_2S@C nanocomposites as high performance cathode materials for lithium–sulfur batteries. *J. Mater. Chem. A* **2017**, *5*, 1428–1433.

[37] Ci, H. N.; Shi, Z. X.; Wang, M. L.; He, Y.; Sun, J. Y. A review in rational design of graphene toward advanced Li–S batteries. *Nano Res. Energy* **2023**, *2*, e9120054.

[38] Zhang, J.; Huang, H.; Bae, J.; Chung, S. H.; Zhang, W. K.; Manthiram, A.; Yu, G. H. Nanostructured host materials for trapping sulfur in rechargeable Li–S batteries: Structure design and interfacial chemistry. *Small Methods* **2018**, *2*, 1700279.

[39] Wang, J. Y.; Yang, N. L.; Tang, H. J.; Dong, Z. H.; Jin, Q.; Yang, M.; Kisailus, D.; Zhao, H. J.; Tang, Z. Y.; Wang, D. Accurate control of multishelled Co_3O_4 hollow microspheres as high-performance anode materials in lithium-ion batteries. *Angew. Chem., Int. Ed.* **2013**, *52*, 6417–6420.

[40] Wang, J. Y.; Tang, H. J.; Zhang, L. J.; Ren, H.; Yu, R. B.; Jin, Q.; Qi, J.; Mao, D.; Yang, M.; Wang, Y. et al. Multi-shelled metal oxides prepared via an anion-adsorption mechanism for lithium-ion batteries. *Nat. Energy* **2016**, *1*, 16050.

[41] Guo, J. C.; Xu, Y. H.; Wang, C. S. Sulfur-impregnated disordered carbon nanotubes cathode for lithium–sulfur batteries. *Nano Lett.* **2011**, *11*, 4288–4294.

[42] Zheng, G. Y.; Yang, Y.; Cha, J. J.; Hong, S. S.; Cui, Y. Hollow carbon nanofiber-encapsulated sulfur cathodes for high specific capacity rechargeable lithium batteries. *Nano Lett.* **2011**, *11*, 4462–4467.

[43] Jin, F. Y.; Xiao, S.; Lu, L. J.; Wang, Y. Efficient activation of high-loading sulfur by small CNTs confined inside a large CNT for high-capacity and high-rate lithium–sulfur batteries. *Nano Lett.* **2016**, *16*, 440–447.

[44] Wang, J. Z.; Lu, L.; Choucair, M.; Stride, J. A.; Xu, X.; Liu, H. K. Sulfur-graphene composite for rechargeable lithium batteries. *J. Power Sources* **2011**, *196*, 7030–7034.

[45] Guo, J. X.; Zhang, J.; Jiang, F.; Zhao, S. H.; Su, Q. M.; Du, G. H. Microporous carbon nanosheets derived from corncobs for lithium–sulfur batteries. *Electrochim. Acta* **2015**, *176*, 853–860.

[46] Liu, H. T.; Liu, F.; Qu, Z. H.; Chen, J. L.; Liu, H.; Tan, Y. Q.; Guo, J. B.; Yan, Y.; Zhao, S.; Zhao, X. S. et al. High sulfur loading and shuttle inhibition of advanced sulfur cathode enabled by graphene network skin and N, P, F-doped mesoporous carbon interfaces for ultra-stable lithium sulfur battery. *Nano Res. Energy* **2023**, *2*, e9120049.

[47] Chen, L.; Liu, Y. Z.; Zhang, F.; Liu, C. H.; Shaw, L. L. PVP-assisted synthesis of uniform carbon coated Li_2S/CB for high-performance lithium–sulfur batteries. *ACS Appl. Mater. Interfaces* **2015**, *7*, 25748–25756.

[48] Sun, D.; Hwa, Y.; Shen, Y.; Huang, Y. H.; Cairns, E. J. Li_2S nano spheres anchored to single-layered graphene as a high-performance cathode material for lithium/sulfur cells. *Nano Energy* **2016**, *26*, 524–532.

[49] Fu, A.; Wang, C. Z.; Pei, F.; Cui, J. Q.; Fang, X. L.; Zheng, N. F. Recent advances in hollow porous carbon materials for lithium–sulfur batteries. *Small* **2019**, *15*, 1804786.

[50] Bi, R. Y.; Zhao, J. L.; Yang, M.; Wang, J. Y.; Yu, R. B.; Wang, D. Multifunctional separator modified with catalytic multishelled structural CoS_2 enables a stable lithium–sulfur battery. *Inorg. Chem. Front.* **2024**, *11*, 8837–8846.

[51] Xu, W.; Bi, R. Y.; Yang, M.; Wang, J. Y.; Yu, R. B.; Wang, D. Hollow multishelled structural TiN as multi-functional catalytic host for high-performance lithium–sulfur batteries. *Nano Res.* **2023**, *16*, 12745–12752.

[52] Li, B.; Wang, J. Y.; Bi, R. Y.; Yang, N. L.; Wan, J. W.; Jiang, H. Y.; Gu, L.; Du, J.; Cao, A. M.; Gao, W. et al. Accurately localizing multiple nanoparticles in a multishelled matrix through shell-to-core evolution for maximizing energy-storage capability. *Adv. Mater.* **2022**, *34*, 2200206.

[53] Mao, D.; Wang, C.; Li, W.; Zhou, L.; Liu, J.; Zheng, Z. J.; Zhao, Y.; Cao, A. M.; Wang, S. T.; Huang, J. X. et al. Hollow multishelled structure: Synthesis chemistry and application. *Chem. Res. Chin. Univ.* **2024**, *40*, 346–393.

[54] Zhao, X. L.; Yang, M.; Wang, J. Y.; Wang, D. Hollow multishelled structural Li-rich cathode with Al doping enabling capacity and voltage stabled Li-ion batteries. *Chem. Res. Chin. Univ.* **2023**, *39*, 630–635.

[55] Wei, Y. Z.; Li, J.; Zhao, D. C.; Zhao, Y. S.; Zhang, Q. H.; Gu, L.; Wan, J. W.; Wang, D. ZnO HoMS@ZIF-8 nanoreactors for efficient enrichment and photoreduction of atmospheric CO_2. *CCS Chem* **2024**, *6*, 3065–3076.

[56] Wang, C.; Wang, X. S.; Yang, Y.; Kushima, A.; Chen, J. T.; Huang, Y. H.; Li, J. Slurryless Li_2S/reduced graphene oxide cathode paper for high-performance lithium sulfur battery. *Nano Lett.* **2015**, *15*, 1796–1802.

[57] Yin, H.; He, J.; Xiao, B.; Zhou, M.; Wang, W.; Cunha, J.; Chen, Z. X.; Hou, Z. H.; Zhang, T. Q.; Yu, Z. P. Advances and prospects of g-C_3N_4 in lithium–sulfur batteries. *Nano Res. Energy* **2024**, *3*, e9120138.

[58] Qiu, Y. C.; Rong, G. L.; Yang, J.; Li, G. Z.; Ma, S.; Wang, X. L.; Pan, Z. H.; Hou, Y.; Liu, M. N.; Ye, F. M. et al. Highly nitridated graphene-Li_2S cathodes with stable modulated cycles. *Adv. Energy Mater.* **2015**, *5*, 1501369.

[59] Zhang, S.; Liu, M. N.; Ma, F.; Ye, F. M.; Li, H. F.; Zhang, X. Y.; Hou, Y.; Qiu, Y. C.; Li, W. F.; Wang, J. et al. A high energy density Li_2S@C nanocomposite cathode with a nitrogen-doped carbon nanotube top current collector. *J. Mater. Chem. A* **2015**, *3*, 18913–18919.

[60] Zhang, J. Q.; Zhou, W.; Zhu, S. S.; Lin, J.; Wei, P. F.; Li, F. F.; Jin, P. P.; Yao, H.; Zhang, Y. J.; Hu, Y. et al. Persistency of enlarged autolysosomes underscores nanoparticle-induced autophagy in hepatocytes. *Small* **2017**, *13*, 1602876.

[61] He, J. R.; Chen, Y. F.; Lv, W. Q.; Wen, K. C.; Xu, C.; Zhang, W. L.; Li, Y. R.; Qin, W.; He, W. D. From metal-organic framework to Li_2S@C–Co–N nanoporous architecture: A high-capacity cathode for lithium–sulfur batteries. *ACS Nano* **2016**, *10*, 10981–10987.

[62] Ruan, J. F.; Sun, H.; Song, Y.; Pang, Y. P.; Yang, J. H.; Sun, D. L.; Zheng, S. Y. Constructing 1D/2D interwoven carbonous matrix to enable high-efficiency sulfur immobilization in Li–S battery. *Energy Mater.* **2021**, *1*, 100018.

[63] Wu, F. X.; Lee, J. T.; Magasinski, A.; Kim, H.; Yushin, G. Solution-based processing of graphene-Li_2S composite cathodes for lithium-ion and lithium–sulfur batteries. *Part. Part. Syst. Charact.* **2014**, *31*, 639–644.

[64] Lin, Z.; Nan, C. Y.; Ye, Y. F.; Guo, J. H.; Zhu, J. F.; Cairns, E. J. High-performance lithium/sulfur cells with a bi-functionally immobilized sulfur cathode. *Nano Energy* **2014**, *9*, 408–416.

[65] Hwa, Y.; Zhao, J.; Cairns, E. J. Lithium sulfide (Li_2S)/graphene oxide nanospheres with conformal carbon coating as a high-rate, long-life cathode for Li/S cells. *Nano Lett.* **2015**, *15*, 3479–3486.

[66] Seh, Z. W.; Wang, H. T.; Liu, N.; Zheng, G. Y.; Li, W. Y.; Yao, H. B.; Cui, Y. High-capacity Li_2S-graphene oxide composite cathodes with stable cycling performance. *Chem. Sci.* **2014**, *5*, 1396–1400.

[67] Han, K.; Shen, J. M.; Hayner, C. M.; Ye, H. Q.; Kung, M. C.; Kung, H. H. Li_2S-reduced graphene oxide nanocomposites as cathode material for lithium sulfur batteries. *J. Power Sources* **2014**, *251*, 331–337.

[68] Wang, D. H.; Xie, D.; Yang, T.; Zhong, Y.; Wang, X. L.; Xia, X. H.; Gu, C. D.; Tu, J. P. Li_2S@C composite incorporated into 3D reduced graphene oxide as a cathode material for lithium–sulfur batteries. *J. Power Sources* **2016**, *313*, 233–239.

[69] Lu, C. W.; Yu, L. Y.; Zhou, X. Z.; Gan, Y. P.; He, X. P.; Huang, H.; Zhang, J.; Zhang, W. K.; Xia, X. H.; Xiao, Z. et al. Li_2S@C/CNT composite cathode with botryoidal conductive network for advanced lithium–sulfur batteries. *J. Solid State Electrochem.* **2024**, *28*, 2413–2423.

[70] Chung, S. H.; Han, P.; Chang, C. H.; Manthiram, A. A shell-shaped carbon architecture with high-loading capability for lithium sulfide cathodes. *Adv. Energy Mater.* **2017**, *7*, 1700537.

[71] Peng, Y. Y.; Zhang, Y. Y.; Wen, Z. P.; Wang, Y. H.; Chen, Z. Q.; Hwang, B. J.; Zhao, J. B. Constructing fast electron and ion conductive framework for Li_2S as advanced lithium sulfur battery. *Chem. Eng. J.* **2018**, *346*, 57–64.

[72] Ye, F. M.; Hou, Y.; Liu, M. N.; Li, W. F.; Yang, X. W.; Qiu, Y. C.; Zhou, L. S.; Li, H. F.; Xu, Y. J.; Zhang, Y. G. Fabrication of mesoporous Li_2S–C nanofibers for high performance Li/Li_2S cell cathodes. *Nanoscale* **2015**, *7*, 9472–9476.

[73] Wu, F. X.; Magasinski, A.; Yushin, G. Nanoporous Li_2S and MWCNT-linked Li_2S powder cathodes for lithium–sulfur and lithium-ion battery chemistries. *J. Mater. Chem. A* **2014**, *2*, 6064–6070.
[74] Wu, M.; Cui, Y.; Fu, Y. Z. Li_2S nanocrystals confined in free-standing carbon paper for high performance lithium–sulfur batteries. *ACS Appl. Mater. Interfaces* **2015**, *7*, 21479–21486.
[75] Zheng, S. Y.; Chen, Y.; Xu, Y. H.; Yi, F.; Zhu, Y. J.; Liu, Y. H.; Yang, J. H.; Wang, C. S. *In situ* formed lithium sulfide/microporous carbon cathodes for lithium-ion batteries. *ACS Nano* **2013**, *7*, 10995–11003.
[76] Zhang, J.; Shi, Y.; Ding, Y.; Peng, L. L.; Zhang, W. K.; Yu, G. H. A conductive molecular framework derived Li_2S/N,P-codoped carbon cathode for advanced lithium–sulfur batteries. *Adv. Energy Mater.* **2017**, *7*, 1602876.
[77] Wang, N.; Zhao, N. Q.; Shi, C. S.; Liu, E. Z.; He, C. N.; He, F.; Ma, L. Y. *In situ* synthesized Li_2S@porous carbon cathode for graphite/Li_2S full cells using ether-based electrolyte. *Electrochim. Acta* **2017**, *256*, 348–356.
[78] Seh, Z. W.; Yu, J. H.; Li, W. Y.; Hsu, P. C.; Wang, H. T.; Sun, Y. M.; Yao, H. B.; Zhang, Q. F.; Cui, Y. Two-dimensional layered transition metal disulphides for effective encapsulation of high-capacity lithium sulphide cathodes. *Nat. Commun.* **2014**, *5*, 5017.
[79] Tao, X. Y.; Wang, J. G.; Liu, C.; Wang, H. T.; Yao, H. B.; Zheng, G. Y.; Seh, Z. W.; Cai, Q. X.; Li, W. Y.; Zhou, G. M. et al. Balancing surface adsorption and diffusion of lithium-polysulfides on nonconductive oxides for lithium–sulfur battery design. *Nat. Commun.* **2016**, *7*, 11203.
[80] Zhou, G. M.; Tian, H. Z.; Jin, Y.; Tao, X. Y.; Liu, B. F.; Zhang, R. F.; Seh, Z. W.; Zhuo, D.; Liu, Y. Y.; Sun, J. et al. Catalytic oxidation of Li_2S on the surface of metal sulfides for Li–S batteries. *Proc. Natl. Acad. Sci. USA* **2017**, *114*, 840–845.
[81] Zhang, K. Y.; Zhao, Z. Q.; Chen, H.; Pan, Y. K.; Niu, B.; Long, D. H.; Zhang, Y. Y. A review of advances in heterostructured catalysts for Li–S batteries: Structural design and mechanism analysis. *Small* **2025**, *21*, 2409674.
[82] Zhang, X.; Bi, R. Y.; Wang, J. Y.; Zheng, M.; Wang, J.; Yu, R. B.; Wang, D. Delicate Co-control of shell structure and sulfur vacancies in interlayer-expanded tungsten disulfide hollow sphere for fast and stable sodium storage. *Adv. Mater.* **2023**, *35*, 2209354.
[83] Wu, R.; Xu, H. K.; Zhao, Y. W.; Zha, C. Y.; Deng, J.; Zhang, C. Y.; Lu, G.; Qin, T. S.; Wang, W.; Yin, Y. et al. Borophene-like boron subunits-inserted molybdenum framework of MoB_2 enables stable and quick-acting Li_2S_6-based lithium–sulfur batteries. *Energy Storage Mater.* **2020**, *32*, 216–224.
[84] He, J. R.; Bhargav, A.; Manthiram, A. High-performance anode-free Li–S batteries with an integrated Li_2S–electrocatalyst cathode. *ACS Energy Lett.* **2022**, *7*, 583–590.
[85] Song, Z. F.; Wang, Z. M.; Yu, R. B. Strategies for advanced supercapacitors based on 2D transition metal dichalcogenides: From material design to device setup. *Small Methods* **2024**, *8*, 2300808.
[86] Du, Y. H.; Liu, Y. H.; Cao, F. F.; Ye, H. Defect-induced-reduced Au quantum dots@MXene decorated separator enables lithium–sulfur batteries with high sulfur utilization. *Energy Mater.* **2024**, *4*, 400014.
[87] Ma, Y. T.; Chang, L. Q.; Yi, D. W.; Liu, M.; Wang, P. C.; Luo, S. L.; Zhang, Z. Y.; Yuan, Y.; Lu, H. Synergetic effect of block and catalysis on polysulfides by functionalized bilayer modification on the separator for lithium–sulfur batteries. *Energy Mater.* **2024**, *4*, 400059.
[88] Raza, H.; Cheng, J. Y.; Wang, J. W.; Kandasamy, S.; Zheng, G. P.; Chen, G. H. Titanium-containing high entropy oxide (Ti-HEO): A redox expediting electrocatalyst towards lithium polysulfides for high performance Li–S batteries. *Nano Res. Energy* **2024**, *3*, e9120116.
[89] Sun, Y. M.; Lee, H. W.; Seh, Z. W.; Zheng, G. Y.; Sun, J.; Li, Y. B.; Cui, Y. Lithium sulfide/metal nanocomposite as a high-capacity cathode prelithiation material. *Adv. Energy Mater.* **2016**, *6*, 1600154.
[90] He, J. R.; Chen, Y. F.; Manthiram, A. Metal sulfide-decorated carbon sponge as a highly efficient electrocatalyst and absorbant for polysulfide in high-loading Li_2S batteries. *Adv. Energy Mater.* **2019**, *9*, 1900584.
[91] Zhao, B.; Ren, Z. X.; Li, Z. S.; Tan, G. Q.; Xie, J. Encapsulate lithium sulfide cathodes with carbon-doped MoS_2 for fast kinetics in lithium–sulfur batteries, a theoretical study. *Acta Mater.* **2023**, *242*, 118441.
[92] Ji, Y. X.; Zhang, J. Y.; Yang, N.; Xue, J. R.; Zhang, W. Y.; He, X. X.; Li, Q.; Lei, Z. B.; Liu, Z. H.; Sun, J. MoC nanoparticles decorated carbon nanofibers loaded with Li_2S as high-performance lithium sulfur battery cathodes. *Appl. Surf. Sci.* **2025**, *679*, 161263.
[93] Seh, Z. W.; Wang, H. T.; Hsu, P. C.; Zhang, Q. F.; Li, W. Y.; Zheng, G. Y.; Yao, H. B.; Cui, Y. Facile synthesis of Li_2S-polypyrrole composite structures for high-performance Li_2S cathodes. *Energy Environ. Sci.* **2014**, *7*, 672–676.
[94] Yang, N.; Xue, J. R.; Ji, Y. X.; Zhang, J. Y.; Zhang, W. Y.; He, X. X.; Li, Q.; Lei, Z. B.; Liu, Z. H.; Sun, J. Self-supporting poly(3,4-ethylenedioxythiophene) and Fe_3C Co-decorated electrospun carbon nanofibers as Li_2S supporters for lithium–sulfur batteries. *Nanoscale* **2025**, *17*, 7877–7887.
[95] Ding, C.; Wang, W. Q.; Zhang, Y. F.; Ding, J. L.; Hou, X. Y.; Jia, Z. C.; Wang, G. C.; Li, C. Z. Mechanochemical construction of fibrous stacked Li_2S cathode with high activity and low tortuosity for anode-free Li–S batteries. *Energy Storage Mater.* **2025**, *79*, 104354.
[96] Zha, C. Y.; Wu, D. H.; Gu, X. Q.; Chen, H. Y. Triple-phase interfaces of graphene-like carbon clusters on antimony trisulfide nanowires enable high-loading and long-lasting liquid Li_2S_6-based lithium–sulfur batteries. *J. Energy Chem.* **2021**, *59*, 599–607.
[97] Aurbach, D.; Pollak, E.; Elazari, R.; Salitra, G.; Kelley, C. S.; Affinito, J. On the surface chemical aspects of very high energy density, rechargeable Li–sulfur batteries. *J. Electrochem. Soc.* **2009**, *156*, A694–A702.
[98] Lin, D. C.; Liu, Y. Y.; Li, Y. B.; Li, Y. Z.; Pei, A.; Xie, J.; Huang, W.; Cui, Y. Fast galvanic lithium corrosion involving a Kirkendall-type mechanism. *Nat. Chem.* **2019**, *11*, 382–389.
[99] Zhang, S. S. Role of $LiNO_3$ in rechargeable lithium/sulfur battery. *Electrochim. Acta* **2012**, *70*, 344–348.
[100] Hou, T. Z.; Xu, W. T.; Chen, X.; Peng, H. J.; Huang, J. Q.; Zhang, Q. Lithium bond chemistry in lithium–sulfur batteries. *Angew. Chem., Int. Ed.* **2017**, *56*, 8178–8182.
[101] Fu, Y. Z.; Manthiram, A. Orthorhombic bipyramidal sulfur coated with polypyrrole nanolayers as a cathode material for lithium–sulfur batteries. *J. Phys. Chem. C* **2012**, *116*, 8910–8915.
[102] Manthiram, A.; Fu, Y. Z.; Chung, S. H.; Zu, C. X.; Su, Y. S. Rechargeable lithium–sulfur batteries. *Chem. Rev.* **2014**, *114*, 11751–11787.
[103] Yang, Y.; Zheng, G. Y.; Cui, Y. A membrane-free lithium/polysulfide semi-liquid battery for large-scale energy storage. *Energy Environ. Sci.* **2013**, *6*, 1552–1558.
[104] Licht, S. Aqueous solubilities, solubility products and standard oxidation-reduction potentials of the metal sulfides. *J. Electrochem. Soc.* **1988**, *135*, 2971–2975.
[105] Barchasz, C.; Leprêtre, J. C.; Patoux, S.; Alloin, F. Electrochemical properties of ether-based electrolytes for lithium/sulfur rechargeable batteries. *Electrochim. Acta* **2013**, *89*, 737–743.
[106] Mikhaylik, Y. V.; Kovalev, I.; Schock, R.; Kumaresan, K.; Xu, J.; Affinito, J. High energy rechargeable Li–S cells for EV application: Status, remaining problems and solutions. *ECS Trans.* **2010**, *25*, 23–34.
[107] Meini, S.; Elazari, R.; Rosenman, A.; Garsuch, A.; Aurbach, D. The use of redox mediators for enhancing utilization of Li_2S cathodes for advanced Li–S battery systems. *J. Phys. Chem. Lett.* **2014**, *5*, 915–918.

[108] Li, Z. H.; Yao, Y. X.; Sun, S.; Jin, C. B.; Yao, N.; Yan, C.; Zhang, Q. 40 Years of low-temperature electrolytes for rechargeable lithium batteries. *Angew. Chem.* **2023**, *135*, e202303888.
[109] Xiao, P. T.; Yun, X. R.; Chen, Y. F.; Guo, X. W.; Gao, P.; Zhou, G. M.; Zheng, C. M. Insights into the solvation chemistry in liquid electrolytes for lithium-based rechargeable batteries. *Chem. Soc. Rev.* **2023**, *52*, 5255–5316.
[110] Asano, H.; Liu, J. L.; Ueno, K.; Dokko, K.; Kojima, T.; Takeichi, N.; Miyuki, T.; Yamakawa, Y.; Watanabe, M. Enhancing the reversibility of Li deposition/dissolution in sulfur batteries using high-concentration electrolytes to develop anode-less batteries with lithium sulfide cathode. *J. Power Sources* **2023**, *554*, 232323.
[111] Lai, T. X.; Bhargav, A.; Reed, S.; Manthiram, A. Long-life graphite-lithium sulfide full cells enabled through a solvent Co-intercalation-free electrolyte design. *Mater. Horiz.* **2025**, *12*, 1282–1289.
[112] Meng, X. Y.; Liu, Y. Z.; Guan, M. T.; Qiu, J. S.; Wang, Z. Y. A high-energy and safe lithium battery enabled by solid-state redox chemistry in a fireproof gel electrolyte. *Adv. Mater.* **2022**, *34*, 2201981.
[113] Meng, X. Y.; Liu, Y. Z.; Wang, Z. Y.; Zhang, Y. Z.; Wang, X. Y.; Qiu, J. S. A quasi-solid-state rechargeable cell with high energy and superior safety enabled by stable redox chemistry of Li_2S in gel electrolyte. *Energy Environ. Sci.* **2021**, *14*, 2278–2290.
[114] Li, Z. N.; Yang, Z. J.; Chhowalla, M. Stabilising graphite anode with quasi-solid-state electrolyte for long-life lithium–sulfur batteries. *MRS Energy Sustain*, in press, DOI: 10.1557/s43581-025-00139-0.
[115] Shin, M.; Gewirth, A. A. Incorporating solvate and solid electrolytes for all-solid-state Li_2S batteries with high capacity and long cycle life. *Adv. Energy Mater.* **2019**, *9*, 1900938.

Wang Xi is currently a graduate student at University of Science and Technology Beijing. He received his B.S. degree in metallurgical engineering from Anhui University of Technology in 2023. His research interests focus on lithium-sulfur batteries.

Song Zhifan is a Ph.D. candidate at the School of Metallurgical and Ecological Engineering, University of Science and Technology Beijing. He received his B.S. degree in metallurgical engineering from the University of Science and Technology Beijing in 2021. His current research interests mainly focus on the controlled synthesis of transition metal sulfide-based nanocomposites and their applications in sodium-ion battery.

Liu Runqiu is currently a graduate student at University of Science and Technology Beijing. He received his B.S. degree in metallurgical engineering from the University of Science and Technology Beijing in 2024. His research interest focuses on alloy-type composite materials for sodium-ion batteries.

Yu Ranbo received her B.S. and M.S. from Jilin University (1994 and 1997) and Ph.D. from Yamanashi University (2002). She worked as a postdoctoral researcher at Kyoto University (JSPS fellow) and the University of Houston in 2002 and 2003. She is currently working as a full professor at the College of Chemistry and Environmental Engineering, Shenzhen University. Her research interests include inorganic materials chemistry and surface chemistry, design, and synthesis of micro-/nanostructured functional materials and their applications in energy conversion and storage.

Wang Jiangyan received her B.E. from the China University of Mining and Technology, Beijing (July 2010) and Ph.D. from the Institute of Process Engineering, Chinese Academy of Sciences (Jan. 2016). Then she worked as a postdoctoral scholar at Stanford University, USA. In 2020, she joined the Institute of Process Engineering, Chinese Academy of Sciences as a professor. Her research interests focus on the design and fabrication of multifunctional heterostructures for energy storage and conversion.